remote sensing

MDPI

Article

A Sustainable Agricultural Development Index (SADI): Bridging Soil Health, Management, and Socioeconomic Factors

Gabriel Pimenta Barbosa de Sousa [1], José Alexandre Melo Demattê [1,2], Sabine Chabrillat [3,4], Robert Milewski [3], Raul Roberto Poppiel [1,2], Merilyn Taynara Accorsi Amorim [1], Bruno dos Anjos Bartsch [1], Jorge Tadeu Fim Rosas [1], Maurício Roberto Cherubin [1], Yuxin Ma [5], Roney Berti de Oliveira [6], Marcos Rafael Nanni [6] and Renan Falcioni [6,*]

[1] Department of Soil Science, Luiz de Queiroz College of Agriculture, University of São Paulo, Pádua Dias Av., 11, P.O. Box 09, Piracicaba 13416-900, SP, Brazil; gabriel1_pimenta@usp.br (G.P.B.d.S.); jamdemat@usp.br (J.A.M.D.); raulpoppiel@usp.br (R.R.P.); merilyn.accorsi@usp.br (M.T.A.A.); brunobartsch@usp.br (B.d.A.B.); jorge.fimrosas@usp.br (J.T.F.R.); cherubin@usp.br (M.R.C.)
[2] Center for Carbon Research in Tropical Agriculture (CCARBON), University of São Paulo, Piracicaba 13416-823, SP, Brazil
[3] Section Remote Sensing and Geoinformatics, Helmholtz Centre for Geosciences GFZ, Telegrafenberg, 14473 Potsdam, Germany; chabri@gfz.de (S.C.); milewski@gfz.de (R.M.)
[4] Soil Science Section, Institute of Earth System Science, Leibniz University Hannover, Herrenhäuser Str. 2, 30419 Hannover, Germany
[5] New South Wales Department of Climate Change, Energy, The Environment and Water, Parramatta 2150, Australia; yuxin.ma@environment.nsw.gov.au
[6] Graduate Program in Agronomy, State University of Maringá, Av. Colombo, 5790, Maringá 87020-900, PR, Brazil; rboliveira@uem.br (R.B.d.O.); mrnanni@uem.br (M.R.N.)
* Correspondence: rfalcioni2@uem.br

Highlights

What are the main findings?

- An index (SADI) integrating soil health, management and economic performance was developed.
- A spatial map revealed critical areas of degradation across Germany.

What is the implication of the main finding?

- SADI supports diagnosing and management strategies for unsustainable agricultural systems
- Healthy soils are associated with higher levels of economic prosperity.

Abstract

Soil Health (SH) is a key concept in discussions on sustainable land use, with implications that extend beyond agriculture. To address the need for integrated assessments, this study developed a Sustainable Agricultural Development Index (SADI) by combining the Soil Health Index (SHI) with socioeconomic and management indicators. The analysis was conducted across Germany using 3300 soil analysis sites and environmental covariates, including climate, topography, vegetation indices, and bare soil reflectance. From this foundation, SADI was designed to evaluate agricultural sustainability across German states based on three dimensions: Management (Bare Soil Frequency), Environment (SHI Maps), and Economy (Profit per Hectare). Results revealed that SHI correlated significantly with land surface temperature (R = −0.47), bare soil frequency (R = −0.40), and vegetation indices (R = 0.43). Soil organic carbon also played a key role in explaining degradation patterns. While economically stronger states tended to achieve higher SH scores, environmentally sound and well-managed regions also performed well despite lower economic

check for updates

Academic Editor: Nicolas Baghdadi

Received: 9 October 2025
Revised: 9 December 2025
Accepted: 11 December 2025
Published: 16 December 2025

Citation: de Sousa, G.P.B.; Demattê, J.A.M.; Chabrillat, S.; Milewski, R.; Poppiel, R.R.; Amorim, M.T.A.; Bartsch, B.d.A.; Rosas, J.T.F.; Cherubin, M.R.; Ma, Y.; et al. A Sustainable Agricultural Development Index (SADI): Bridging Soil Health, Management, and Socioeconomic Factors. *Remote Sens.* **2025**, *17*, 4039. https://doi.org/10.3390/rs17244039

Copyright: © 2025 by the authors. Licensee MDPI, Basel, Switzerland. This article is an open access article distributed under the terms and conditions of the Creative Commons Attribution (CC BY) license (https://creativecommons.org/licenses/by/4.0/).

returns. These findings emphasize that sustainable agriculture depends on balancing economic growth, environmental integrity, and management efficiency. The SADI provides a comprehensive framework for policymakers and land managers to evaluate and guide sustainable agricultural development.

Keywords: soil quality; soil degradation; agricultural effectiveness; digital soil mapping; artificial intelligence; environmental sustainability

1. Introduction

Approximately 95% of global food production depends on healthy soils, yet nearly one-third of the world's soils are already degraded [1]. This degradation is largely driven by unsustainable land use practices—such as intensive agriculture, deforestation, and urban expansion—which have transformed 30–50% of Earth's land surface [2]. These pressures accelerate erosion, reduce nutrient stocks, and diminish biodiversity, compromising ecosystem resilience. With the global population projected to reach 9.7 billion by 2050 and food demand expected to rise by up to 60% [3,4], maintaining soil sustainability has become a central challenge for global food security and environmental stability.

Soil Health (SH) has emerged as a unifying framework to address this challenge. Defined as the capacity of soil to function as a living ecosystem that sustains plants, animals, and humans [5], SH encompasses multiple ecological processes: supporting crop production, regulating water flow and quality, cycling nutrients, storing carbon, and hosting diverse biological communities [5,6]. Unlike traditional notions of soil quality, which often focus narrowly on productivity, SH promotes a holistic view that emphasizes long-term ecological functioning and the provision of ecosystem services [6–8]. Because SH integrates biological, chemical, and physical properties that vary with environmental, social, and management conditions, advancing it requires an interdisciplinary perspective [9].

Despite this holistic mandate, the role of pedology and geology in shaping SH remains underexplored in contemporary SH assessments [10]. Several studies have shown that parent material, mineralogy, and soil-forming processes exert first-order controls over texture, nutrient availability, pH, cation-exchange capacity, and soil organic carbon—properties that directly influence the functional capacity of soils [11–13]. However, the broader SH literature has historically emphasized management-driven changes while giving comparatively less attention to inherent soil-forming factors, making pedogenesis remain insufficiently integrated into modern SH frameworks [14]. Understanding geological and pedological context is therefore crucial for distinguishing degradation caused by management from patterns that arise from natural soil variability.

Recent progress in remote sensing (RS) and machine learning (ML) has made it possible to monitor soil and land conditions over large areas with increasing precision [15]. Satellite observations provide repeatable information on vegetation cover, greenness, land surface temperature, and proxies related to soil condition [15,16]. Combined with ML algorithms, these datasets have been used to predict soil attributes and land degradation indicators. For instance, Poppiel et al. (2025) [17] generated a 90 m Soil Health Index (SHI) map for Latin America, illustrating the potential of RS-based approaches to identify patterns of soil function across broad regions. Other studies have linked vegetation dynamics and hydrological responses to SH-related processes [18,19]. These advances demonstrate the value of RS as a cost-effective tool for large-scale soil monitoring.

However, important limitations remain. RS primarily captures surface properties and therefore detects soil degradation only indirectly [20]. Subtle changes, such as declines

in soil organic matter (SOM) or biological activity—may not produce immediate spectral responses and often go unnoticed until vegetation is visibly affected. Additionally, Digital Soil Mapping (DSM) faces structural constraints related to soil sampling: analysis dates are rarely recorded systematically, creating heterogeneous datasets that hinder the modeling of temporal soil dynamics [21,22]. As a result, most models represent soil conditions as static snapshots rather than temporally explicit processes.

A further gap concerns the limited integration of socio-economic and management factors. While RS indicators effectively highlight where degradation or suboptimal SHI occurs, they do not explain why it occurs. Human-driven factors, such as land use decisions, input management, and economic constraints, play a central role in shaping soil conditions, yet they are not directly observable from satellite imagery [23]. Without these dimensions, SHI maps risk being diagnostically rich but operationally limited. Integrating environmental, economic, and management information is therefore essential to produce assessments that better inform policy interventions and sustainable agricultural planning [24].

Building on this limitation, there is currently no consolidated framework that simultaneously integrates soil condition, ecosystem service provision, economic productivity, and management practices into a single operational indicator. This gap motivates the development of the Sustainable Agricultural Development Index (SADI) proposed in this study. SADI combines RS and ML soil proxies with profitability metrics and land use management, capturing how ecological processes interact with socio-economic performance. Whereas the SHI concentrates on the biophysical dimensions of soil functioning, SADI extends the analytical scope to include human-driven factors that fundamentally shape agricultural outcomes. By incorporating these additional dimensions, the SADI offers a more comprehensive and decision-relevant measure of sustainable agricultural development.

The objectives of this study are to: (i) produce the first national-scale, spatially explicit SHI for Germany using digital soil mapping and uncertainty analysis; (ii) validate the SHI through RS indicators and independent European degradation datasets; (iii) develop the SADI by integrating soil functioning, management intensity, and economic performance; (iv) evaluate its interpretability across contrasting German states while assessing whether functional soil attributes remain coherent across SADI classes. Through this framework, we aim to provide a proof-of-concept for SADI as a robust tool to support sustainable food systems and resilient landscapes.

2. Material and Methods

2.1. Study Area

The study area encompasses the entire Germany territory (357,168 km^2). Additionally, a 100 km buffer around the perimeter was included to incorporate surrounding points (BSO), thereby improving mapping accuracy along the edges. The terrain ranges from its lowest point at 3.54 m below sea level in Neuendorf-Sachsenbande to its highest point in Bavaria at 2.96 m. The climate is predominantly temperate (Cfb), with temperatures varying from −5 °C in winter to 30 °C in summer [25].

2.2. Pedological and Geological Datasets Incorporated into SHI Interpretation

To contextualize spatial patterns observed in the SHI, national pedological and geological datasets were integrated into the analysis. Pedological information was obtained from the BGR Soil Map of the Federal Republic of Germany at 1:1,000,000 scale [26], which provides the national distribution of WRB soil groups across the country. This dataset delineates the predominant soil types across the entire Germany territory.

Geological parent material information was sourced from the BGR—"Grupen der Bodenausgangsgesteine in Deutschland" at 1:5,000,000 scale [27], which identifies major lithological units such as sandy cover deposits, loess and loess derivatives, and claystones.

Both datasets were converted to raster format and resampled to match the spatial resolution and projection of the SHI layers (90 m). For each grid cell, the dominant pedological class and parent material category was assigned based on maximum area overlap. These layers were subsequently used to stratify SHI values and examine their spatial distribution across contrasting pedological and geological settings.

2.3. Land Uses Separation

To better understand the behavior of the SHI across Germany, we divided the country into three broad land use regions: anthropogenic, agricultural, and forest, defined by their land cover characteristics [28]. The anthropogenic areas (ANSO) encompass locations strongly influenced by human activities other than agriculture (e.g., mining sites, urban and industrial areas). Given the distinct role of food production, we separated agricultural areas (AGSO) into their own category despite being human influenced, to provide more detailed information about agricultural soil conditions. Areas with minimal direct human impact were classified as forest areas (FSO), representing predominantly natural landscapes.

2.4. Soil Site Observations

We used a legacy database compiled from two main sources: the LUCAS (Land Use/Cover Area Frame Statistical Survey) dataset and a private soil database developed by researchers at the GFZ German Research Centre for Geosciences (Table 1). All observations were subjected to a standardized filtering procedure to ensure consistency and analytical reliability. First, we assessed the accuracy of geographic coordinates and removed duplicated records with identical locations. Next, we evaluated the availability of each modeled attribute, discarding missing values only for the specific parameter while retaining each sample for all other measured properties.

Table 1. Number of soil observations before and after the filtering.

Soil Attribute	Original Soil Observations	BSO (100 km)	ANSO (3.3×10^6 ha)	AGSO (2×10^7 ha)	FSO (1.1×10^7 ha)	Filtered Soil Observations
Physicals						
Bulk Density (BD)	404	201	2	141	60	389
Clay	2638	715	37	1508	378	2537
Biologicals						
Soil Organic Carbon (SOC)	2836	715	39	1704	378	2595
Chemicals						
Potassium (K)	2604	715	37	1478	378	2370
Nitrogen (N)	2608	715	37	1478	378	2394
Cation-exchange Capacity (CEC)	2608	715	37	1478	378	2458
Phosphorus (P)	2608	711	37	1478	378	2428
pH	2608	715	37	1478	378	2507

In the case of bulk density (BD), both databases contained only a limited number of observations. This scarcity of data imposes an inherent constraint on the predictive modeling, as models tend to underperform when trained on poorly represented attributes.

Even so, all available BD measurements were retained to maximize the representation of this parameter in the modeling process.

We also harmonized the measurement units across datasets, ensuring that each soil property was expressed using a consistent metric (e.g., cmolc/dm^3 or mmolc/dm^3). Finally, we verified methodological compatibility by selecting only samples analyzed using comparable laboratory protocols, for example, the same analytical method for pH determination.

2.5. Environmental Covariates (EC)

To map all attributes contributing to the SHI (Table 1), we selected 34 EC as predictors. The SHI is a single metric designed to represent variations in soil conditions that support ecosystems of similar nature (e.g., biomes or micro-regions). These EC were chosen for their significance in the soil formation process [29] and their connection to the impact of human activities on landscape changes. They were obtained from diverse sources (Table 2).

Table 2. Environmental covariates used for modeling attributes.

Factors	EC	Unit	Source (Spatial Resolution)	References
Climatic	AMT	°C	WorldClim BIO Variables V1 (90 m)	[30]
	TAR	°C	WorldClim BIO Variables V7 (90 m)	[30]
	AP	mm	WorldClim BIO Variables V12 (90 m)	[30]
	PS	mm	WorldClim BIO Variables V15 (90 m)	[30]
Relief	Elevation	Meter	SRTM (90 m)	[31]
	Slope	Degree	TAGEE/SRTM (90 m)	[31]
	Aspect	Degree	TAGEE/SRTM (90 m)	[31]
	Hillshade	Dimensionless	TAGEE/SRTM (90 m)	[31]
	Northness	Dimensionless	TAGEE/SRTM (90 m)	[31]
	Eastness	Dimensionless	TAGEE/SRTM (90 m)	[31]
	Horizontal Curvature	Meter	TAGEE/SRTM (90 m)	[31]
	Vertical Curvature	Meter	TAGEE/SRTM (90 m)	[31]
	Mean Curvature	Meter	TAGEE/SRTM (90 m)	[31]
	Gaussian Curvature	Meter	TAGEE/SRTM (90 m)	[31]
	Minimal Curvature	Meter	TAGEE/SRTM (90 m)	[31]
	Maximal Curvature	Meter	TAGEE/SRTM (90 m)	[31]
	Shape Index	Dimensionless	TAGEE/SRTM (90 m)	[31]
	MultiScale Topographic Position Index	Meter	TAGEE/SRTM (90 m)	[31]
	Euclidean Distance to Water		TAGEE/SRTM (90 m)	[31]
Soil + Vegetation	SYSI Blue (450–520 nm)	-	Landsat collection (90 m)	[32]
	SYSI Green (520–600 nm)	-	Landsat collection (90 m)	[32]
	SYSI Red (630–690 nm)	-	Landsat collection (90 m)	[32]
	SYSI NIR (760–900 nm)	-	Landsat collection (90 m)	[32]
	SYSI SWIR1 (1550–1750 nm)	-	Landsat collection (90 m)	[32]
	SYSI SWIR2 (2080–2350 nm)	-	Landsat collection (90 m)	[32]
	mBlue (450–520 nm)	-	Landsat collection (90 m)	In this study
	mGreen (520–600 nm)	-	Landsat collection (90 m)	In this study
	mRed (630–690 nm)	-	Landsat collection (90 m)	In this study
	mNIR (760–900 nm)	-	Landsat collection (90 m)	In this study

Table 2. *Cont.*

Factors	EC	Unit	Source (Spatial Resolution)	References
Soil + Vegetation	mSWIR1 (1550–1750 nm)	-	Landsat collection (90 m)	In this study
	mSWIR2 (2080–2350 nm)	-	Landsat collection (90 m)	In this study
Soil activity	Mode Land Use and Coverage	-	Sentinel & Landsat collections (90 m)	[28]
Vegetation	EVI	-	Landsat collection (90 m)	In this study
	SAVI	-	Landsat collection (90 m)	In this study
Land Surface Temperature (LST)	LST	Kelvin	Landsat collection (90 m)	[33]

Annual Mean Temperature (AMT); Temperature Annual Range (TAR); Annual Precipitation (AP); Precipitation Seasonality (PS); Synthetic Soil Image (SYSI); Terrain Analysis in Google Earth Engine (TAGEE); Shuttle Radar Topography Mission (SRTM). Land Surface Temperature (LST); Bands of mean Vegetation Reflectance (mBlue, mGreen, mRed, mNIR, mSWIR1, mSWIR2); Vegetation indexes—EVI (Enhanced Vegetation Index), SAVI (Soil Adjusted Vegetation Index).

Given that our modeling framework intentionally excludes the temporal dynamics of soil attributes and assumes a fixed reference time, we standardized all predictor rasters to represent a "current" generalized state. To achieve this, we computed the mean of the available historical records for climate variables, soil and vegetation indices, and land surface temperature, thereby producing temporally aggregated layers that mitigate year-to-year variability. Topographic data were treated as time-invariant, under the assumption that elevation and terrain derivatives exhibit negligible change over the temporal span of the datasets used.

For land use and land cover, which often present substantial short-term fluctuations, we adopted the modal class across the time series. This approach identifies the most persistent land use signal at each location, ensuring that the predictor reflects the dominant anthropogenic or natural pressure likely influencing the measured soil attribute.

2.5.1. Soil Environmental Covariates

To represent the soil factor in modeling and predicting tasks, we employed two key products:

i. Following the methodology proposed by [32], we used the Geospatial Soil Sensing System (GEOS3) to produce the Synthetic Soil Image (SYSI) which represents the bare soil across German over the entire image collection period from 1982 to 2023. This image represents the mean reflectance of bare soil and includes six spectral bands: Blue (band 1), Green (band 2), Red (band 3), NIR (band 4), SWIR1 (band 5), and SWIR2 (band 6). This product has proven to be efficient and been widely used in studies focusing on correlation analysis and prediction of soil attributes [32,34,35].
ii. Relief factors were incorporated as soil covariates. These variables were generated using the TAGEE methodology proposed by [31], which derives terrain attributes from a 30 m resolution digital elevation model (DEM) obtained from the Shuttle Radar Topography Mission (SRTM). For consistency with other datasets, all terrain attributes were resampled to a spatial resolution of 90 m.

2.5.2. Vegetation, Climatic, Ground Cover Activity Covariates

Despite the significant agricultural activity in Germany, several natural areas remain in the territory. For regions where the soil has never been exposed and therefore cannot be analyzed remotely, we use covariates that provide indirect soil information through vegetation analysis [36]. Additionally, we use traditional vegetation indices to enhance our

set of predictive covariates, such as Enhanced Vegetation Index (EVI) and Soil Adjusted Vegetation Index (SAVI).

We collected from the WorldClim BIO V1 dataset [30], which provides a global average (1970–2000) climate series with a 1 km spatial resolution, data about national temperature and precipitation patterns to derive climate variables. These include mean annual temperature (MAT), annual precipitation (AP), temperature annual range (TAR) defined as the difference between the hottest and coldest day of the year—and seasonal precipitation (PS). These climatic covariates were resampled to a spatial resolution of 90 m.

Land Surface Temperature (LST) was obtained from the thermal band (band 10) of Landsat 8 images on the Google Earth Engine (GEE) platform, using a cloud mask developed from QA_Pixel band, and calculated using the methods proposed by [33]. The data was then aggregated to represent the median LST for the period from 1985 to 2023 across the entire German territory.

Based on the temporal information on land use and cover provided by the European Environmental Agency (EEA, 2018) [28], we calculated the mode of use and cover of German soils between 2000 and 2018. The resulting product can identify areas that were primarily agricultural territories, which consequently show greater trends of high presence of chemical attributes such as N, P and K.

2.6. Soil Attributes Mapping

Soil attributes were mapped at a 90 m spatial resolution for the 0–20 cm layer using a geospatial mapping pipeline fully developed in Python (v3.10) on the Google Colab platform and integrated with GEE. The modeling process began with the extraction of EC values at sampling locations to build the training dataset. We then performed hyperparameter tuning for the Random Forest algorithm, evaluating 27 different model configurations per soil attribute.

To assess model performance, we applied 10-fold stratified cross-validation based on the distribution of the target variable by biome, calculating performance metrics. The best model for each attribute was selected according to the lowest RMSE value. To evaluate the effect of spatial autocorrelation on model performance, we further applied spatial leave-one-out cross-validation (SLOO-CV) using buffer distances of 10, 100, 1000, 2000, and 5000 m.

Once the optimal models were selected, spatial predictions were generated across the study area using stratified resampling by biome through 100 bootstrap iterations. The final output included spatial maps of mean predictions, standard error, and the 5th and 95th percentiles (prediction intervals) for each soil attribute in the 0–20 cm layer, all at a 90 m spatial resolution.

2.7. SH Assessment and Mapping

The SH assessment followed three steps:

(i) selecting a minimum dataset.
(ii) interpreting measured indicators.
(iii) integrating indicators into an overall index, as outlined by [37] and widely accepted in global literature [38,39].

Our dataset included seven soil indicators: pH, P, K, Ca, CEC, BD, and SOC (Figure 1). These indicators represent the chemical, physical, and biological components of soil. According to [5], a comprehensive SHI should include a balanced set of biological, physical, and chemical indicators. To enhance the representation of the biological component, we incorporated an earthworm abundance map, derived from a global model [40]. While SOC has often been used as a proxy for biological activity, the inclusion of earthworm

data provides a more direct and functionally meaningful measure of biological processes. Earthworms are widely recognized as key indicators of soil biological quality due to their role in SOM decomposition, nutrient cycling, and soil structure maintenance [41]. These indicators address multiple soil functions and ecosystem services, such as plant production, nutrient cycling, carbon sequestration, water regulation, erosion mitigation, and habitat provision for soil biota [5,37,42,43].

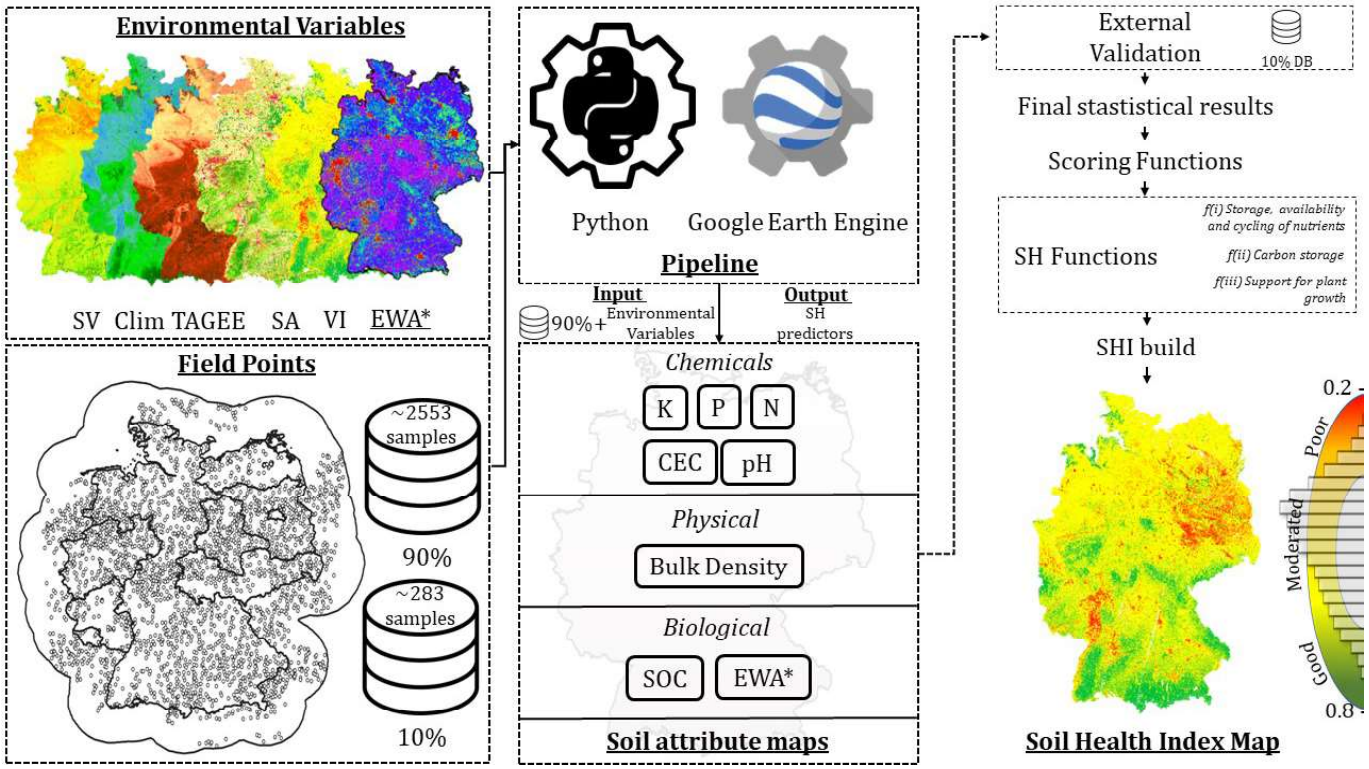

Figure 1. Workflow for mapping SHI in Germany soils. SV: Bands of mean Vegetation Reflectance; Relief (TAGEE); SA: Land use and Coverage; VI: Vegetation Index; EWA*: Earthworms abundance—not used for the soil attributes map modeling, only used to compose the biological parameters of SH functions.

Following the approach previously applied in SH assessments [37], each soil indicator was scored according to its contribution to agronomic performance and environmental regulation. Three types of scoring functions were used:

(i) "more is better" (MBI), represented by an upper asymptote sigmoid function, applied when higher values improve SH.
(ii) "less is better" (LBI), modeled with a lower asymptote sigmoid curve, used when lower values indicate improved conditions.
(iii) "optimal midpoint" (OMI), represented by a Gaussian function, where intermediate values reflect ideal SH conditions.

In this study, K, P, CEC, N and SOC were scored using the MBI function, as elevated levels of these indicators are typically associated with higher soil fertility and biological activity. BD was evaluated using the LBI function, since lower values reflect better physical conditions for root development. Soil pH in water (pH_H_2O) was scored using the OMI function, as extreme pH values (either too acidic or alkaline) are generally detrimental to plant growth, and an intermediate value is considered optimal.

The non-linear Equations (1) and (2) were used for scoring attributes following the MBI and LBI patterns, respectively. For attributes with an OMI, Equations (3) and (4) were applied to the left and right sides of the Gaussian curve.

$$Score = \frac{a}{\left[1 + \left(\frac{LB-UT}{x-UT}\right)^{S}\right]} \quad (1)$$

$$Score = \frac{a}{\left[1 + \left(\frac{LB-LT}{x-LT}\right)^{S}\right]} \quad (2)$$

$$Score = \frac{a}{\left[1 + \left(\frac{LB-O}{x-O}\right)^{S}\right]} \quad (3)$$

$$Score = \frac{a}{\left[1 + \left(\frac{UB-O}{x-O}\right)^{S}\right]} \quad (4)$$

In these equations, *Score* is the unitless value assigned to the soil attribute, ranging from 0 to 1; a is the maximum score value (set to 1 in this study); x is the observed value of the soil indicator; S is the slope factor, fixed at -2.5 to control curve steepness; *LT* and *UT* are the lower and upper thresholds, respectively; *LB* represents the lower baseline of the optimal range curve, corresponding to a score of 50%, while *UB* denotes the upper baseline, also associated with a score of 50%; and *O* is the optimal value in the case of OMI. Thresholds and baseline values were determined from a national soil database, using the 1st and 99th percentiles as lower and upper limits and the median to define baseline values.

Finally, the third step integrates the indicators into a *SHI*, using the weighted additive approach (Equation (5)),

$$SHI = \sum_{i=1}^{n} S_i W_i \quad (5)$$

where *SHI* is calculated based on the scores of individual indicators (*Si*), considering a total of n integrated indicators. Each indicator is assigned a specific weight (*Wi*).

The SHI was composed of three functions:

f(i), related to the storage, availability and cycling of nutrients, was further divided into three sub-functions.

f(ii), addressed carbon storage, while function.

f(iii) focused on support for plant growth.

Soil indicators were allocated to each respective function or sub-function. The weights assigned to each indicator and sub-function are presented in Table 3, based on expert opinion and the relevant literature [17,37]. Therefore, within each function, numerical weights were assigned to each indicator based on their assumed relevance to the specific soil function or sub-function. This weighting approach is well-established in the literature [34,37,44,45].

2.8. Validation Strategy for SHI

2.8.1. Uncertainty Assessment of Soil Attribute Proxies

The first component of the SHI validation consisted of evaluating the uncertainty associated with the SH proxies used to estimate the ecosystem functions aggregated in the index. For each predicted soil attribute, the standard deviation of model outputs was calculated to quantify epistemic uncertainty and identify spatial regions where variability may influence the robustness of the SHI. In addition to this uncertainty analysis, further proxy-validation strategies were implemented to assess the internal coherence of

the predicted soil attributes. Specifically, spatial relationships known to be pedologically consistent were examined, including the relationship between clay content and CEC, the spatial correspondence between SOC and N, and the C/N ratio within agricultural areas. These evaluations provided an additional internal check on the plausibility of attribute predictions prior to their integration into the final SHI.

Table 3. Soil functions framework and indicators used to develop the SHI.

Index	Soil Function	Weight	Sub-Functions	Weight	Indicators		Scoring Function	Scoring-Curve Shape
					1st Level	Weight		
SHI	f(i)	0.34	f(i.i)	0.4	P	0.33	MBI	
					K	0.33	MBI	
					N	0.33	MBI	
			f(i.ii)	0.4	pH	1	OMI	
			f(i.iii)	0.2	CEC	1	MBI	
	f(ii)	0.33			SOC	0.5	MBI	
					Earthworms	0.5	MBI	
	f(iii)	0.33			Bulk Density	1	LBI	

f(i): Storage, availability and cycling of nutrients; f(i.i): Nutrient availability; f(i.ii): Acidity/Al toxicity; f(i.iii): Nutrient storage and cycling; f(ii): Carbon storage; f(iii): Support for plant growth.

2.8.2. Spatial and Statistical Correlation with RS Sustainability Indicators

To assess the ecological coherence of the SHI, the index was compared with independent RS indicators known to represent key soil–vegetation and soil–management interactions. Specifically, the Normalized Difference Vegetation Index (NDVI), Bare Soil Frequency (BSF), and SOC were harmonized to the spatial resolution and agricultural mask of the SHI. Pearson correlation coefficients and corresponding *p*-values were computed to quantify expected associations, such as positive relationships with NDVI and SOC and negative relationships with BSF, thereby evaluating whether SHI gradients align with established ecological and agronomic patterns.

2.8.3. Correlation with Independent European Soil Degradation Products

External validation was performed using two soil degradation products from the European Soil Data Centre (ESDAC) (Table 4). The first dataset represents European degradation threats derived from multiple environmental and management indicators. The second dataset is a multiband raster containing 20 spatial indicators of soil degradation, environmental risks, and ecological stress. Both products were resampled to the SHI

projection and resolution, and correlations were computed between the SHI and each band individually. This evaluation aimed to determine whether areas with lower SHI coincide with regions identified as degraded or vulnerable across Europe, thus providing an external benchmark for the index.

Table 4. Description of the bands included in the two ESDAC products used for external validation of the German Soil Health Index (SHI).

ESDAC Product	Description	Bands
European Soil Degradation Indicators	[46]	Bands 1–12
Multiband Soil Degradation Indicators	[47]	Bands 1–20

For European Soil Degradation Indicators, the 12 bands represent major European soil degradation threats provided by ESDAC, including: water erosion (Band 1), wind erosion (Band 2), soil organic carbon loss (Band 3), salinization (Band 4), acidification (Band 5), soil compaction (Band 6), nutrient imbalances (Band 7), pesticide contamination (Band 8), heavy-metal contamination (Band 9), vegetation degradation (Band 10), groundwater decline (Band 11), and aridity (Band 12). For Multiband Soil Degradation Indicators, the 20-band raster comprises quantitative indicators of environmental stress, degradation, and soil functional risk, including: arsenic (Band 1), cadmium (Band 2), copper (Band 3), mercury (Band 4), nitrogen surplus (Band 5), phosphorus deficiency (Band 6), phosphorus excess (Band 7), soil compaction (Band 8), peatland degradation risk (Band 9), post-fire recovery (Band 10), harvest erosion (Band 11), secondary salinization risk (Band 12), potential threat to biological functions (Band 13), distance to maximum SOC level (Band 14), soil sealing (Band 15), tillage erosion (Band 16), water erosion (Band 17), wind erosion (Band 18), zinc (Band 19), and a synthetic index representing the sum of all indicators (Band 20).

2.9. Creation of the SADI

To finalize the Sustainable Agricultural Development Index (SADI), we based our formulation on three core components: the economic factor (EcF), the environmental factor (EnF), and the management factor (MnF). These parameters were integrated into an equation (Equation (6)) with predefined weights that produce the final index, calculated exclusively for AGSO areas to ensure that the assessment focused on regions directly involved in agricultural production. Using the established equation and the processed predictor layers, the SADI was computed for each German state to derive a national ranking of sustainable agricultural development.

The assignment of weights to the three pillars was performed empirically, guided by the conceptual foundation of sustainable development and by the intended purpose of the index. Because SH constitutes the fundamental dimension underpinning long-term agricultural sustainability, the environmental component received the highest weight (0.5). This reflects the assumption that changes in soil conditions exert the strongest influence on sustainability trajectories. The management dimension, quantified through BSF, was assigned an intermediate weight (0.3), as management practices directly shape soil functioning and the overall performance of agroecosystems. Finally, although economic conditions are essential for the feasibility and adoption of sustainable strategies, the economic factor was assigned to a comparatively lower weight (0.2), acknowledging its influence while preserving the centrality of environmental integrity in sustainability assessments.

$$SADI = (EnF \times 0.5) + (MnF \times 0.3) + (EcF \times 0.2) \quad (6)$$

2.9.1. Economic, Environmental and Management Factors

To assess the EcF, we focused on measuring how efficiently financial resources are being utilized in agricultural production at the state level. For this purpose, profit per hectare was selected as the key indicator, as it reflects the return on investment in a standardized way. A higher profit per hectare indicates more efficient and productive use of financial inputs [48].

As a way of representing the EnF, defined as how preserved or degraded the environment is, we simply used the SHI developed on this study. For each state, the average

SHI was established, with the aim of obtaining an understanding of soil conservation in Germany.

The BSF was used as a proxy for MnF. This choice was based on its ability to differentiate between conventional and no-tillage systems, as demonstrated by [49].

2.9.2. Validation Strategy for the SADI

The validation of the SADI was carried out through a multi-layered approach that integrates the independent validation of its component factors, the assessment of internal coherence between environmental functions, and a contextual comparative analysis between contrasting agricultural regions. Because the SADI is constructed from three established components—SHI, BSF, and EcF—its reliability is inherently linked to the robustness and interpretability of these constituent variables.

Independent Validation of SADI Components

The SHI component was validated separately through uncertainty analysis, spatial correlation with RS indicators, and external comparison with European soil degradation datasets, ensuring that its contribution to SADI is grounded in biophysical evidence. The BSF component has well-documented ecological and agronomic implications, with strong empirical support linking soil exposure to erosion risk, degradation processes, and unsustainable land management [32,50–52]. Finally, the economic factor (EcF) is derived from official statistical records of agricultural profit per hectare, representing an objective and externally verifiable economic measure for each German state.

Internal Consistency Assessment Using SHI Functional Components

To complement these independent validations and avoid circularity in evaluating the SADI through its own weighted pillars, we incorporated an assessment based on the three unweighted functional components of the SHI (chemical, physical, and biological soil functions). The rationale is that a region with high SADI values should not only express strong economic and management performance but also be supported by soils that maintain a balanced expression of key ecosystem functions.

For each spatial unit, we extracted the three SHI functional scores and computed their standard deviation, treating this metric as an indicator of functional imbalance. Lower standard deviation values indicate that chemical, physical, and biological functions are expressed symmetrically, whereas higher values signal disproportionate contributions and reduced multifunctionality. This evaluation allows us to test whether regions with higher SADI tend to coincide with soils that are not only healthier in magnitude but also more functionally balanced. As such, this step serves as an additional internal-consistency check for SADI, using an independent dimension of soil functioning that is not integrated into the SADI weighting scheme.

To operationalize this analysis at the landscape scale, the continuous SADI raster was further stratified into three classes—Low, Moderate, and Good sustainability levels—using the 25th and 75th percentiles (Q1 and Q3) of the national SADI distribution. Values below the 25th percentile were assigned to the Low class, values between the 25th and 75th percentiles to the Moderate class, and values above the 75th percentile to the Good class. This classification ensured that comparisons of soil functional balance were made across statistically distinct SADI groups. The SHI-based imbalance metric (standard deviation of chemical, physical, and biological functions) was then summarized within each SADI class, enabling the evaluation of whether higher SADI levels coincide with soils exhibiting greater functional equilibrium.

Contextual and Explanatory Comparative Analysis

Although each SADI component is validated independently, an additional contextual step was implemented to evaluate whether the integrated index captures coherent patterns of sustainable agricultural development. To this end, we conducted a comparative analysis between two states that historically exhibit contrasting agricultural, economic, and management trajectories—Rheinland-Pfalz and Sachsen-Anhalt. By examining whether these well-known structural divergences align with the SADI outcomes, we assess the extent to which the index reflects real-world agricultural development dynamics.

This contextual/explanatory evaluation does not serve as a direct quantitative test of model performance, rather, it provides a validation of plausibility and convergence, verifying whether SADI patterns are consistent with independently recognized socioeconomic, management, and land use histories.

3. Results

3.1. Physical-Chemical-Biological Territorial Understanding

Currently, Germany lacks national-scale spatial maps that provide detailed chemical, physical, and biological soil information. Therefore, it is necessary to produce each of the maps individually to compose the SHI (Figure 2). We obtained statistically significant results (R^2 ranging from 0.39 to 0.63). The clay and CEC maps showed regionally distinct peak patterns. Additionally, the SOC and N maps revealed a strong correlation, reflecting SOC dynamics and enabling SHI validation improves through the C/N ratio [53].

3.2. Uncertainty of Soil Attribute Predictions

To support the reliability of the soil functions used to construct the SHI, we evaluated the spatial uncertainty of each underlying soil attribute (Figure 3). Prediction uncertainty, expressed as the standard deviation across model outputs, showed heterogeneous patterns across Germany, with locally higher values in regions with complex soil transitions or limited training data availability. On average, uncertainty ranged from low values for pH (≈10%) and bulk density (≈13.6%) to substantially higher values for P (≈44.5%), K (≈43.5%), CEC (≈33.7%) and SOC (≈31.7%) reflecting differences in attribute variability and model sensitivity. These patterns provide an additional diagnostic layer supporting the interpretation of the SHI.

3.3. Germany SH Assessment

From the spatialized indicators, we created the SHI map (Figure 4) that mainly com-posed the SADI. German soils are mostly composed of AGSO (60%), followed by ANSO (28%) and FSO (12%)—(Figure 4). This scenario corroborates SHI concentrated in a median classification, in which almost 80% of the soils are in a moderate situation. The more degraded the soil, the greater the tendency for land use to follow a pattern of increasing ANSO and decreasing FSO. On the other hand, high SHI values indicate a significantly higher proportion of AGSO and FSO in relation to ANSO. We divided the German territory based on SHI classifications—poor (P), moderate (M), and good (G)—and analyzed the land use patterns within each category. In general, in areas with low and moderate SHI, ANSO and AGSO were predominant compared to FSO. Conversely, in regions with high SHI, FSO exceeded ANSO, despite a significant predominance of AGSO.

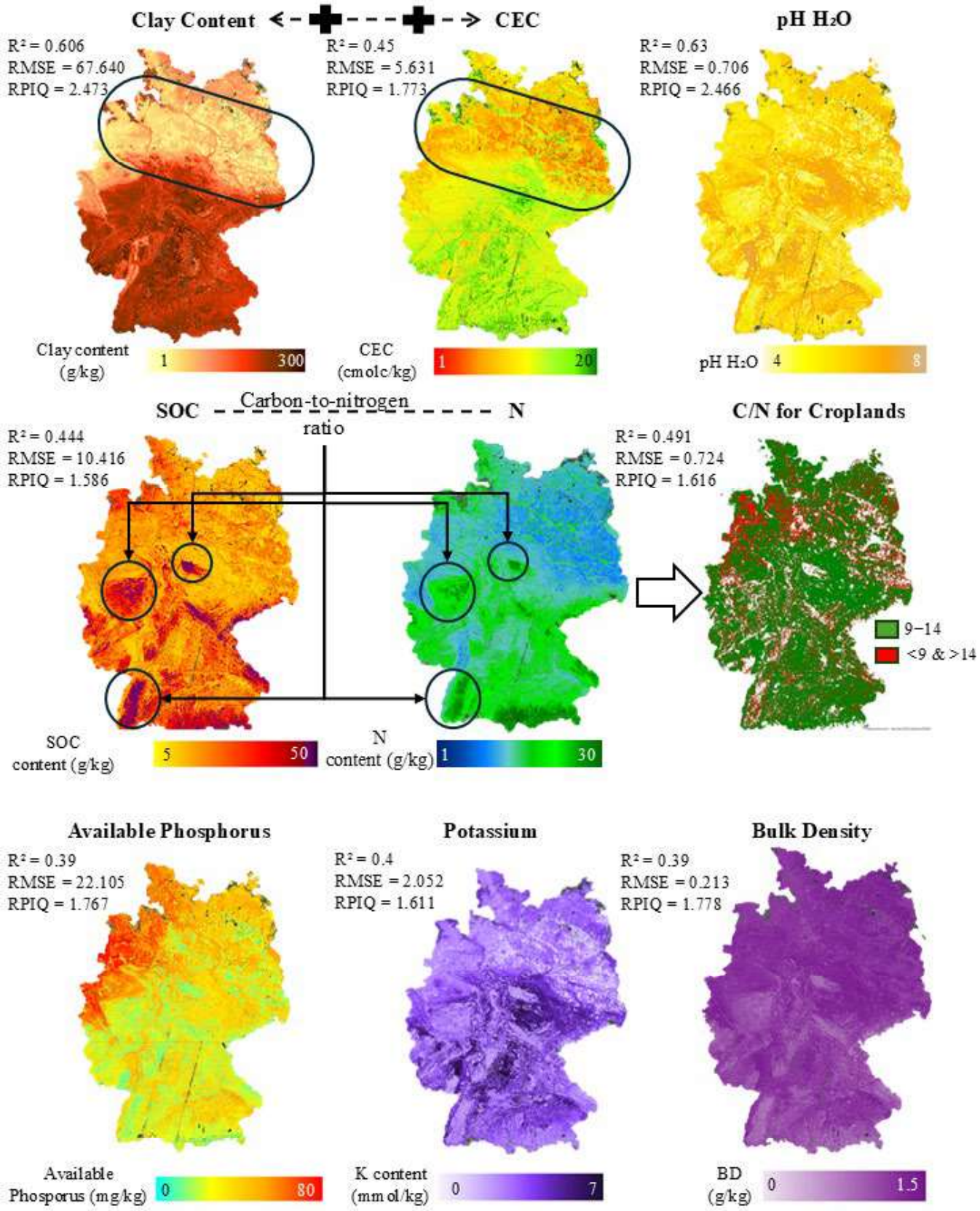

Figure 2. Soil attribute maps modeled to compose the SHI equation.

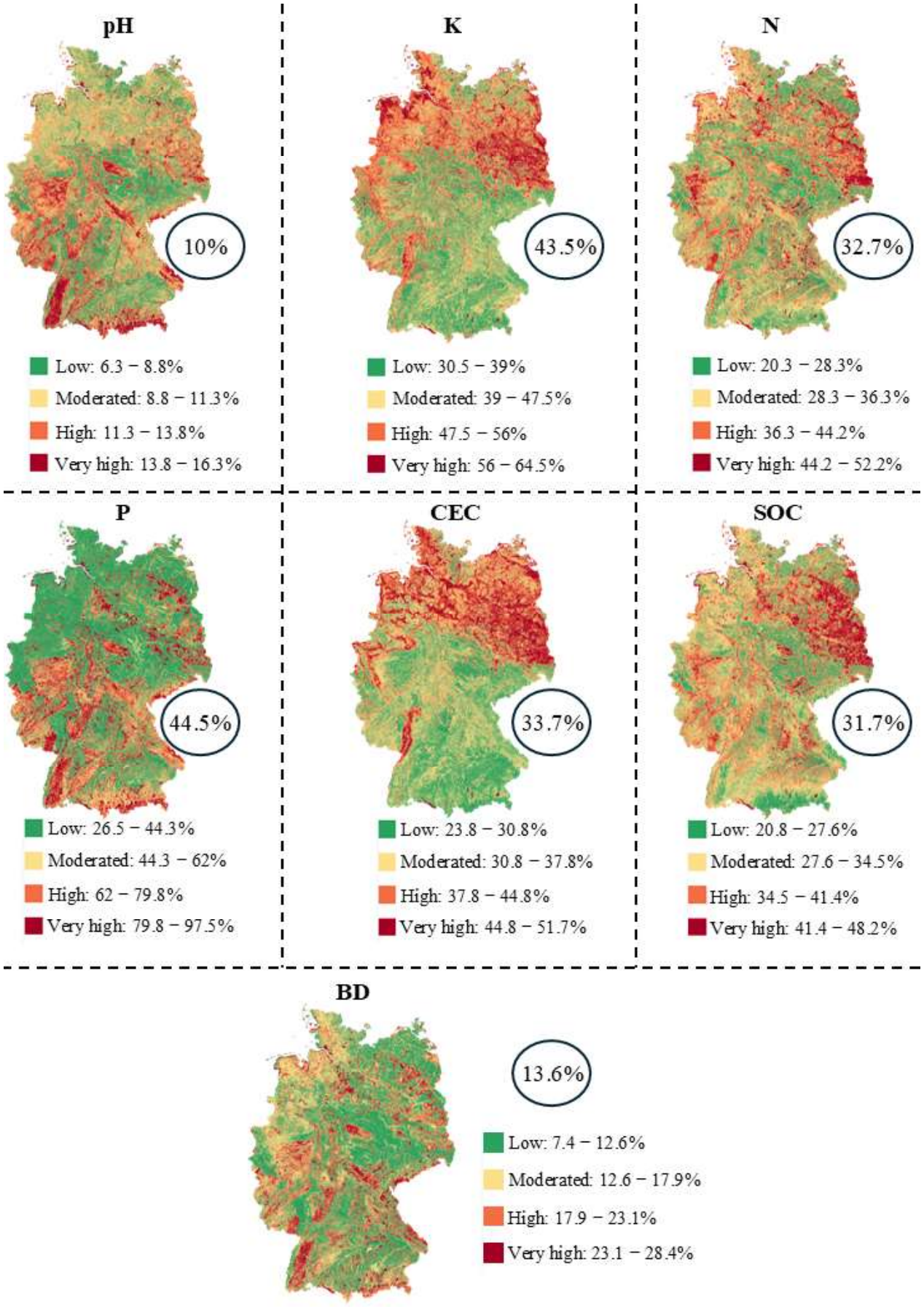

Figure 3. Spatial uncertainty of the predicted soil attributes used to construct the SHI across Germany.

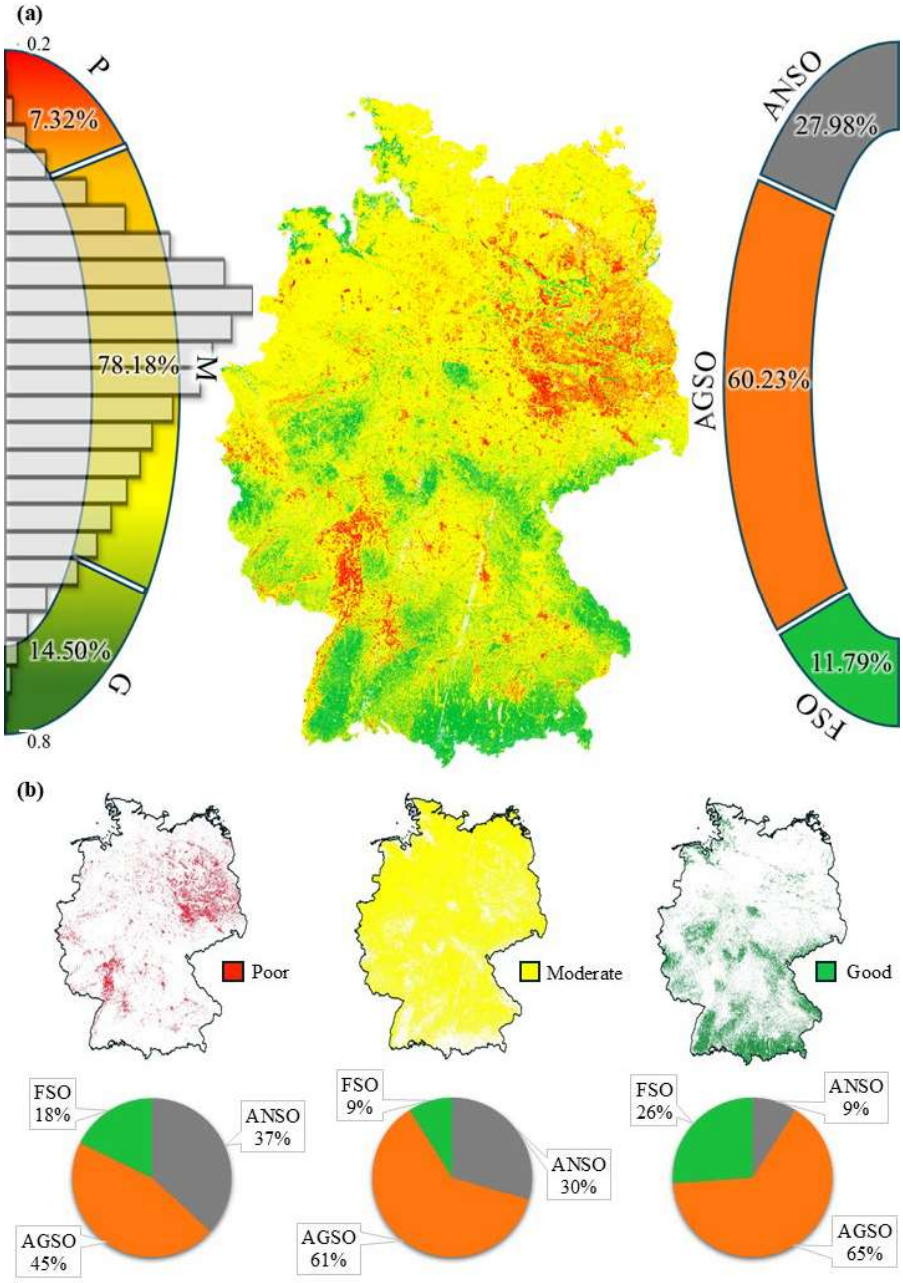

Figure 4. Spatial distribution of SHI and LUC distribution across Germany. (**a**) represents the SHI distribution and the percentage of land use areas across the entire territory. (**b**) represents the SHI classes distribution based on the % of LUC area.

3.4. SHI Validation Based on RS Indicators

To evaluate the ecological consistency of the SHI, we compared its spatial patterns with independent RS indicators representing vegetation vigor (NDVI), soil exposure (BSF), and modeled organic matter status (SOC map). Two representative regions with contrasting SHI values were selected to examine whether high and low SH exhibited the expected environmental signatures (Figure 5). Areas classified as healthy soils showed substantially higher NDVI (0.35 vs. 0.24), lower BSF (4.7% vs. 17.5%), and markedly higher SOC (43.0 vs. 15.9 g/kg), while unhealthy areas displayed the opposite trends. These contrasts confirm that SHI gradients align with well-established ecological relationships, where healthier soils support greater vegetative cover, accumulate more SOC, and exhibit reduced surface exposure. This convergence across independent datasets strengthens the external validity of the SHI.

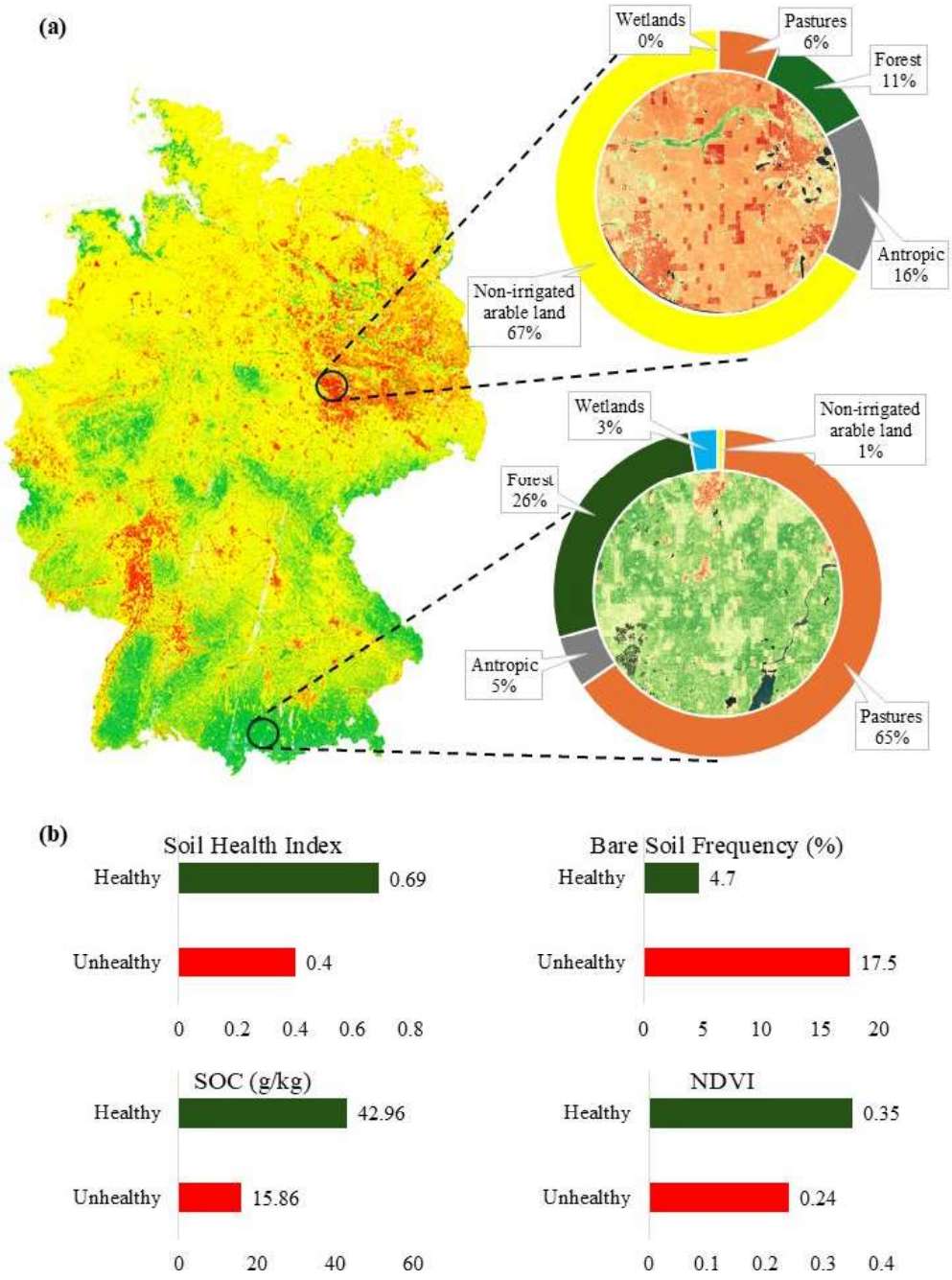

Figure 5. SHI validation factors. (**a**) the analyzed areas composed of low SHI and high SHI and their LUC. (**b**) validation factors value for each area.

3.5. External Validation Against Independent European Soil Degradation Products

Although several correlations were statistically significant, many absolute values were moderate to low ($R < 0.20$ for a substantial portion of the bands), reflecting the heterogeneous and multi-process nature of the ESDAC indicators. As shown in Figure 6, the distribution of correlation values captures the conceptual and spatial mismatch between continental-scale degradation indicators and the soil functions represented in the SHI. Among the 20-band multiband product, strong negative correlations were observed for post-fire recovery ($r = -0.47$), peatland degradation risk ($r = -0.34$), and distance to maximum SOC level ($r = -0.26$), indicating that areas with lower SHI correspond to zones identified as highly vulnerable or degraded in continental-scale assessments. Conversely, a small group of indicators exhibited weak positive correlations with the SHI, including

soil pollution by heavy metals (r = 0.23), zinc (r = 0.16), water erosion (r = 0.17), and potential biological-function threats (r = 0.12). These positive associations do not reflect causal improvements in SH; instead, they highlight conceptual and spatial mismatches between these ESDAC products and the functional dimensions represented in the SHI. Several of these indicators capture geological background concentrations (e.g., zinc, some heavy metals), landscape-scale hydrological erosion potential, or broad ecological risk categories that do not directly align with soil function processes at the SHI resolution. As such, these correlations should be interpreted as methodological limitations rather than evidence of ecological convergence.

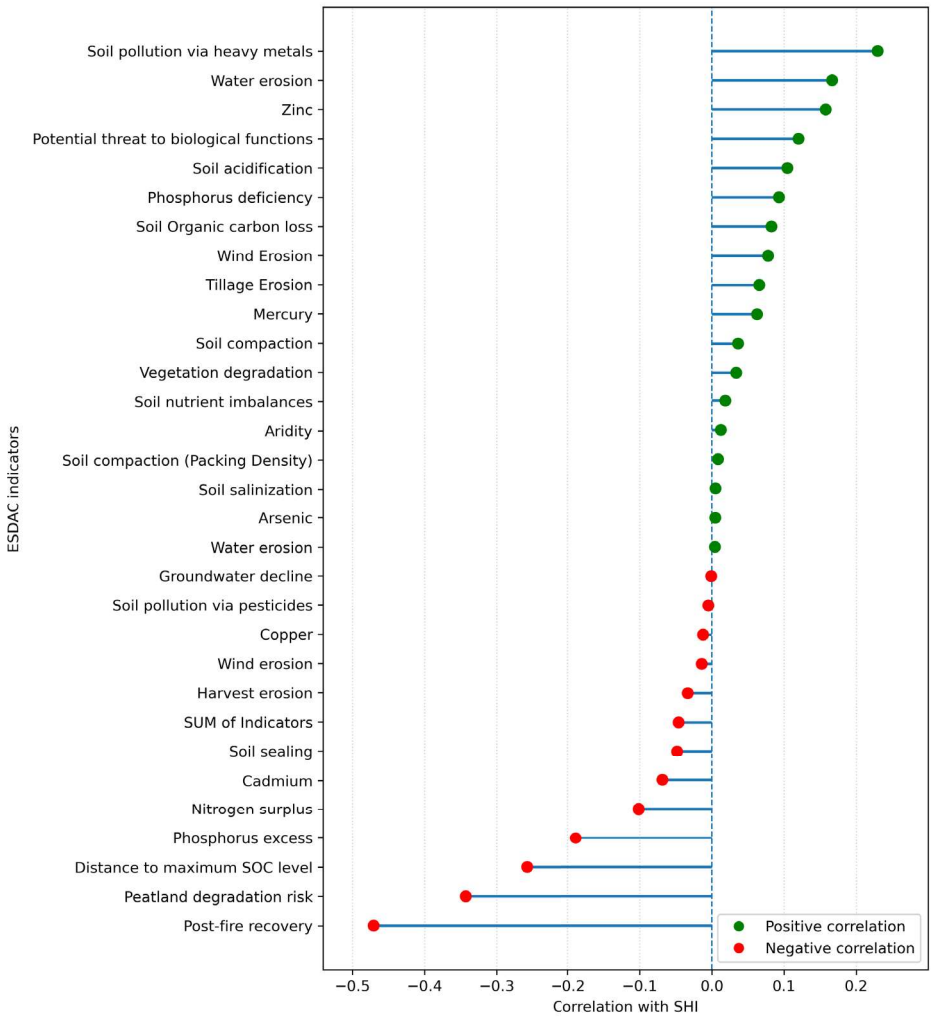

Figure 6. Correlation between the Soil Health Index (SHI) and independent soil degradation indicators from the European Soil Data Centre (ESDAC).

3.6. Soil and Geological Context of SHI Variations

Pedological soil types are classified into Anthrosols, Podzols, Luvisols, Gleysols, Fluvisols, and Cambisols (Figure 7a). Geological formations are grouped into human-altered zones, sandy layers, loess deposits and their derivatives, clay, and rocks (Figure 7b). Each bar represents the area occupied by FSO, ANSO, and AGSO, while the lines show the SHI for each soil category. The highlighted icons illustrate naturally poor and fertile soils. The dotted line represents the overall SHI averaged, while the solid lines indicate the specific SHI for FSO, ANSO, and AGSO. A trend of higher SHI is evident in FSO and Cambisol, contrasting with lower SHI in Podzols and sandy layers.

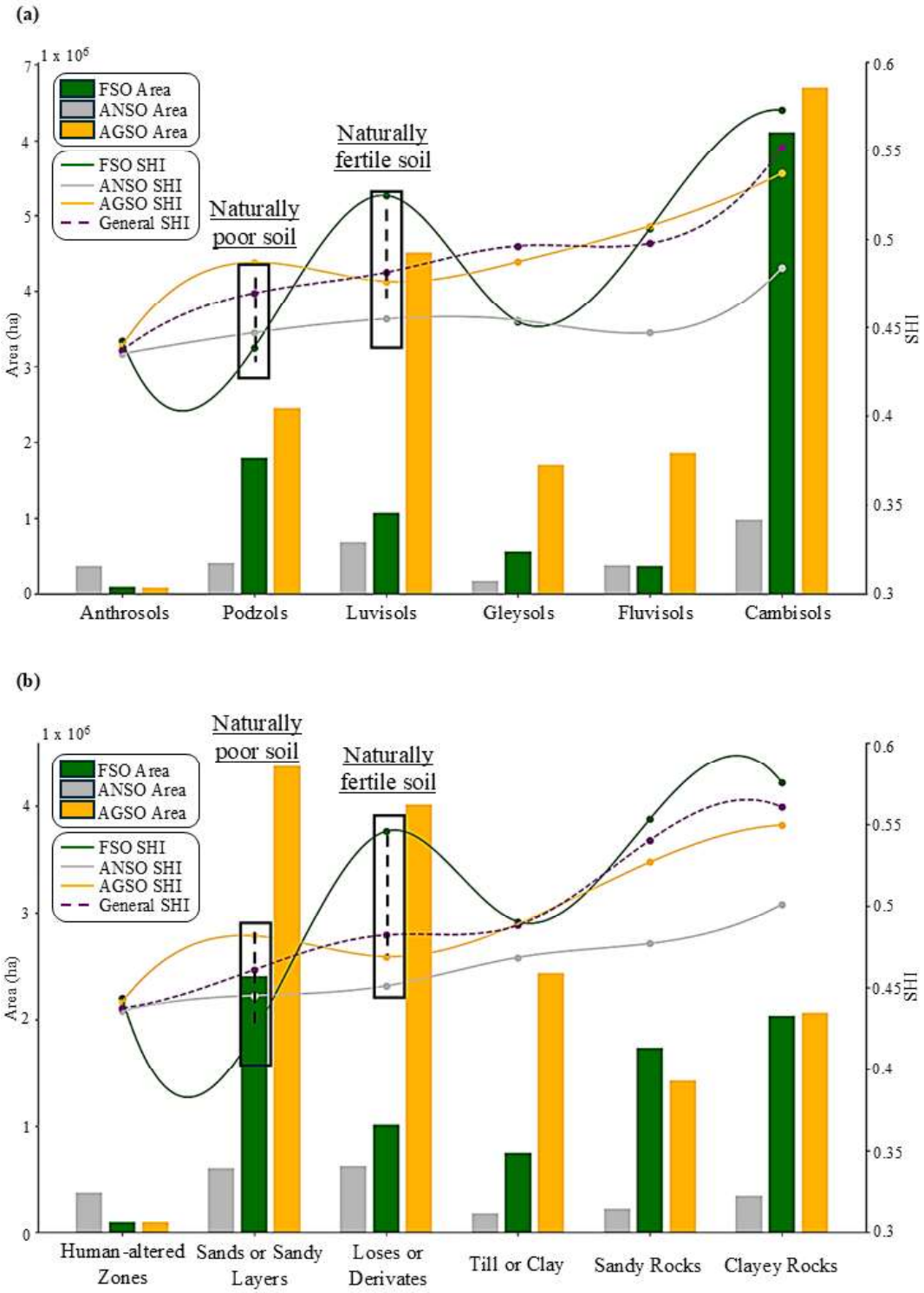

Figure 7. Relationship between SHI, Pedological Classes (**a**) and Geology (**b**). The rectangles with dashed lines represent the difference between the SHI of ANSO and FSO.

3.7. Sustainable Agricultural Development Index (SADI)

A national ranking was established, divided by state, to assess the efficiency and sustainability of agricultural production in the German states (Table 5). Table 5 underscores the importance of a multifactorial analysis in defining optimal scenarios for agricultural production. Saarland, for instance, excels in management practices, which is also reflected positively in environmental indicators. However, despite this performance, Saarland does not rank at the top due to its low agricultural profitability. In contrast, Sachsen-Anhalt

ranks at the bottom, showing the poorest levels in management, SH, and a significant economic fragility in its agricultural sector. It is important to note that the three German city-states—Berlin, Hamburg, and Bremen—were excluded from the ranking. These units possess negligible rural or cropland areas and together account for less than 0.1% of the national agricultural GDP, making their inclusion irrelevant for evaluating agricultural sustainability. Therefore, only states with meaningful agricultural activity were considered.

Table 5. Final rank of the SADI. * Colors on a scale from green to red represent the best to worst performance on sustainable agricultural development.

State *	MnF	EnF	EcF	SADI
Rheinland-Pfalz	0.93	0.43	1.00	0.66
Nordrhein-Westfalen	0.92	0.44	0.86	0.65
Bayern	0.91	0.46	0.81	0.64
Baden-Württemberg	0.93	0.47	0.68	0.62
Niedersachsen	0.94	0.39	0.66	0.59
Saarland	0.97	0.51	0.13	0.56
Schleswig-Holstein	0.94	0.41	0.34	0.55
Hessen	0.92	0.44	0.32	0.53
Sachsen	0.85	0.40	0.12	0.47
Thüringen	0.84	0.39	0.07	0.46
Mecklenburg-Vorpommern	0.85	0.35	0.03	0.43
Brandenburg	0.86	0.32	0.00	0.41
Sachsen-Anhalt	0.83	0.30	0.04	0.40

3.8. Functional Equilibrium of Soil Functions Across SADI Classes

The three SHI soil functions showed a consistent increase from the Poor to the Good SADI class (Figure 8a). Carbon storage increased from 0.44 to 0.52, plant-growth support from 0.37 to 0.48, and nutrient storage and cycling from 0.55 to 0.64. These patterns indicate that higher SADI levels coincide with higher absolute soil-function scores.

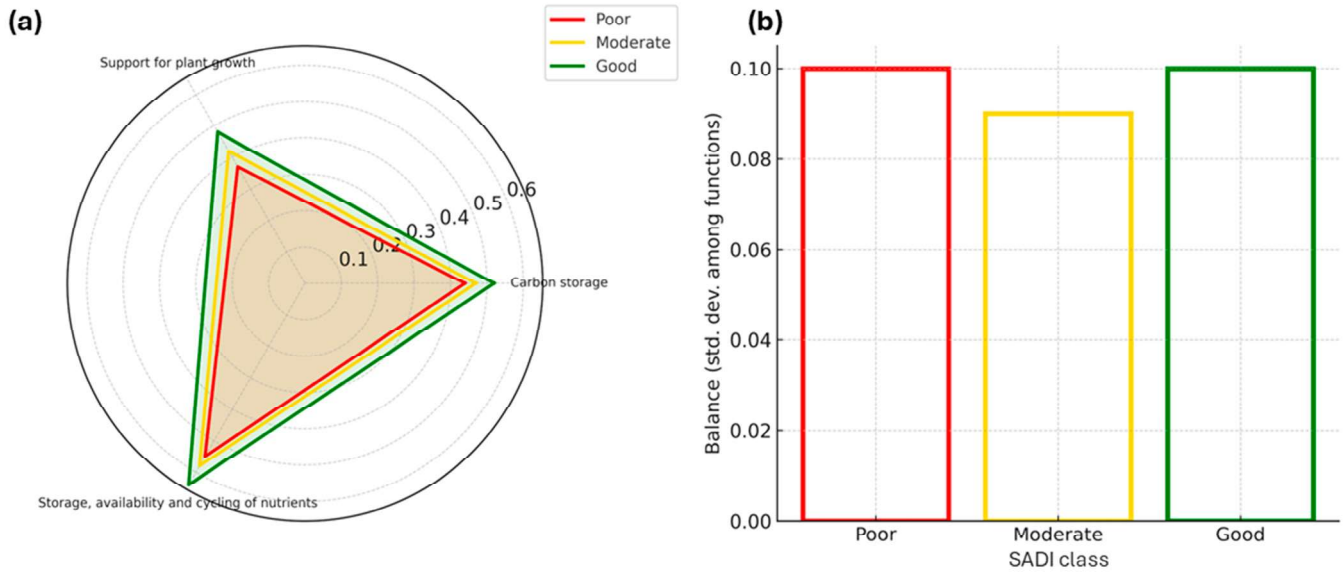

Figure 8. Functional soil attributes and their balance across SADI classes. (**a**) Radar plots showing the mean values of the three SHI soil functions, stratified by SADI classes. (**b**) Functional balance across SADI classes, expressed as the standard deviation among the three soil functions.

The functional balance, expressed as the standard deviation among the three soil functions, remained nearly constant across classes (0.10 for Poor, 0.09 for Moderate, and

0.10 for Good) (Figure 8b). This shows that, although the magnitude of soil functions increases with SADI, the relative equilibrium among chemical, physical, and biological functions does not substantially differ among classes.

4. Discussion

4.1. Spatial Distribution and Relationships Between Soil Attributes in Germany

The spatial distribution of soil attributes in Germany (Figure 2) reveals patterns closely linked to pedological, climatic, and agricultural practices. We observe that the soil attributes made possible to understand the dynamics of German soils chemical and physical interactions in different regions of the country.

Soil exhibits constant dynamism, where the elements found within it are directly related. Clay content, CEC, SOC, and N are classic physical and chemical soil factors that have a clear interconnection, widely discussed in soil science [54–57]. Encompassing two of the main descriptive pillars of soils (physical and chemical), an intrinsic relationship between clay and CEC contents was noted (Figure 2). The high clay content in specific areas, such as in the central-east and south, is characteristic of regions with higher water and nutrient retention, contributing to greater natural soil fertility [58]. These patterns can be attributed to the geological formation of Germany, where the south predominantly consists of carbonate rocks, primarily mixed and carbonate sedimentary rocks. In contrast, the north encompasses extensive areas of sandstone, mainly unconsolidated sediments, and siliciclastic sedimentary rocks [59]. Soils with higher clay content generally exhibit higher CEC due to the greater surface area of particles and their ability to adsorb cations, in addition to the presence of high activity minerals, such as smectites and illites [60]. However, this relationship is complex, as not all clay fractions have the same CEC potential. For example, 2:1 clay has a higher CEC than 1:1, such as kaolinite [61]. Additionally, SOC influences CEC due to its high capacity for cation retention [57]. In this context, we mapped SOC, and when visually comparing, similar patterns can be observed between the SOC and CEC maps. SOC shows a varied distribution, with higher levels in areas with clay-rich soils and regions that practice conservation agriculture, such as cover cropping and no-till farming. The influence of clay and SOC on soil CEC has long been debated. We also found similar behavior of SOC and N which can be explained by the strong correlation between these elements as they are both integral components of organic compounds [62,63]. As SOC accumulates in certain areas, N levels also tend to increase, reflecting their co-occurrence in OM. In soils rich in SOC, microorganisms have more organic material to decompose, which releases N over time. This continuous process of decomposition contributes to maintaining high concentrations of both SOC and N in the same areas. Soils with higher SOC levels are typically more fertile, retaining moisture and nutrients more effectively, which promotes the accumulation of both SOC and N [64]. This pattern highlights the role of SOC as a common indicator of soil fertility and nutrient availability. Liu et al. (2012) [65] observed a strong correlation coefficient (R) of 0.93 between SOC and N in their study. Several authors have also examined how the conversion of natural environments to agricultural land influences SOC-related properties in European soils [66–68]. Similarly, Matschullat et al. (2018) [69], in a review of European soils, found results consistent with those obtained in our work, with average C/N ratios in German agricultural soils ranging from 9 to 14.

When these spatial gradients are interpreted jointly with the prediction–uncertainty maps (Figure 3), it becomes clear that not all regions contribute equally to the robustness of the modeled patterns. The aggregated uncertainty metrics indicate that K, CEC and SOC are the least certain attributes (43.5, 33.7 and 31.7%, respectively), whereas pH and BD show substantially lower overall uncertainty (10 and 13.6%). Spatially, the highest uncertainty for K, CEC, SOC and N is concentrated in the northern lowlands and parts of central–eastern

Germany, where glacial and fluvio-glacial sediments, heterogeneous land use and strong environmental gradients have long been recognized as challenging settings for DSM [70]. This pattern mirrors the behavior reported for LUCAS-based continental products, in which prediction errors and confidence intervals are typically larger in sandy northern Germany and in geomorphologically complex belts than in the loess- and carbonate-dominated south [71,72].

Soil pH shows moderate variation across the country, with generally low values (primarily attributed to the high concentration of SiO_2), representing the sandy sediments from the last glaciation period [73]. Amid the median values, slightly more acidic soils are found in the northwest, while more basic soils are in the central regions. Liming practices in agricultural areas have helped maintain pH levels suitable for crop productivity. Muller et al. (2022) [74] focused on mapping the soil pH of Germany and found a similar pattern. More acidic regions (pH < 5) were in the northwest due to acidic parent material, while soils with a more basic pH (>7) were concentrated in the central-southern region, characterized by loess and carbonate-rich soils. P shows variability related both to soil acidity and agricultural management. Clayey and acidic soils tend to have lower P availability, while more neutral soils exhibit higher concentrations of this essential nutrient, often intensified using phosphate fertilizers [36]. The distribution of P across the territory is largely influenced by anthropogenic fertilization in agricultural areas, with higher concentrations found in cultivated regions. The geological and pedogenic context does not play a major role in P levels, making climatic and management factors the main drivers of P behavior in Germany [75].

Uncertainty patterns for pH and P reinforce these interpretations. While pH exhibits predominantly low to moderate uncertainty across most of the territory (Figure 3), the P map indicates moderate uncertainty concentrated mainly in the central and southern agricultural belts. This pattern is consistent with the behavior reported for plant-available P in European digital soil mapping, where uncertainty tends to be moderate—and spatially clustered—due to the strong influence of historical fertilization, short-range variability, and legacy effects of manure application rather than broad regional gradients [72,76,77]. Consequently, although P uncertainty is not uniformly high, regions with moderate uncertainty still require caution when the map is used for fine-scale nutrient recommendations, as management-induced heterogeneity can lead to substantial sub-field variation that cannot be fully captured by national-scale DSM products.

K and BD also display specific patterns. K, crucial for plant growth, follows a pattern that can be explained by soil texture and fertilizer application. In general, clay-rich soils have a greater capacity to retain K, leading to a similar spatial distribution between the two maps [72]. Soil BD is higher in compacted areas, often associated with intensive agricultural practices and heavy machinery traffic. This is evident in some of the country's agricultural regions, where soil compaction can limit root development and water infiltration.

The interaction between soil attributes is evident in the relationship between clay content, CEC, SOC, and N. Soils rich in clay and SOC tend to have higher fertility and a greater capacity to support high-yield agricultural production. However, the balance among these attributes relies heavily on proper management and the preservation of SH. This underscores the need for sustainable practices that maintain SOC levels, enhance nutrient retention capacity, and ensure long-term productivity.

From a broader perspective, the joint analysis of spatial patterns and their associated uncertainties emphasizes that soil maps for Germany should not be interpreted as deterministic surfaces, but as predictions with spatially varying confidence. This interpretation is in line with recent reviews on digital soil mapping that highlight the risks of ignoring uncertainty when using soil products in environmental modeling and decision

support [78,79]. For national indicators such as the SHI and SADI, areas combining coherent attribute patterns with low to moderate uncertainty provide the most reliable basis for inference, whereas regions with high uncertainty—particularly in northern and central transitional landscapes—should be priority targets for future field campaigns, integration of proximal sensing (e.g., spectroscopy) and model refinement [80,81]. Such efforts would reduce structural knowledge gaps and improve the long-term robustness of soil-health and sustainability assessments in Germany.

4.2. Bare Soil Frequency (BSF) and Land Surface Temperature (LST) on SH Degradation

The degradation of SH is a multifactorial process that can be intensified by inappropriate management practices, such as the intensive use of conventional tillage systems (CTS), which leave bare soil and promote erosive processes and fertility loss [82]. In agreement with our findings (Figure 9), the BSF has proven to be a valuable index for monitoring this degradation, particularly when analyzed alongside LST. These results corroborate previous studies [83,84], which highlight the synergy between BSF and LST as key indicators for identifying areas susceptible to degradation.

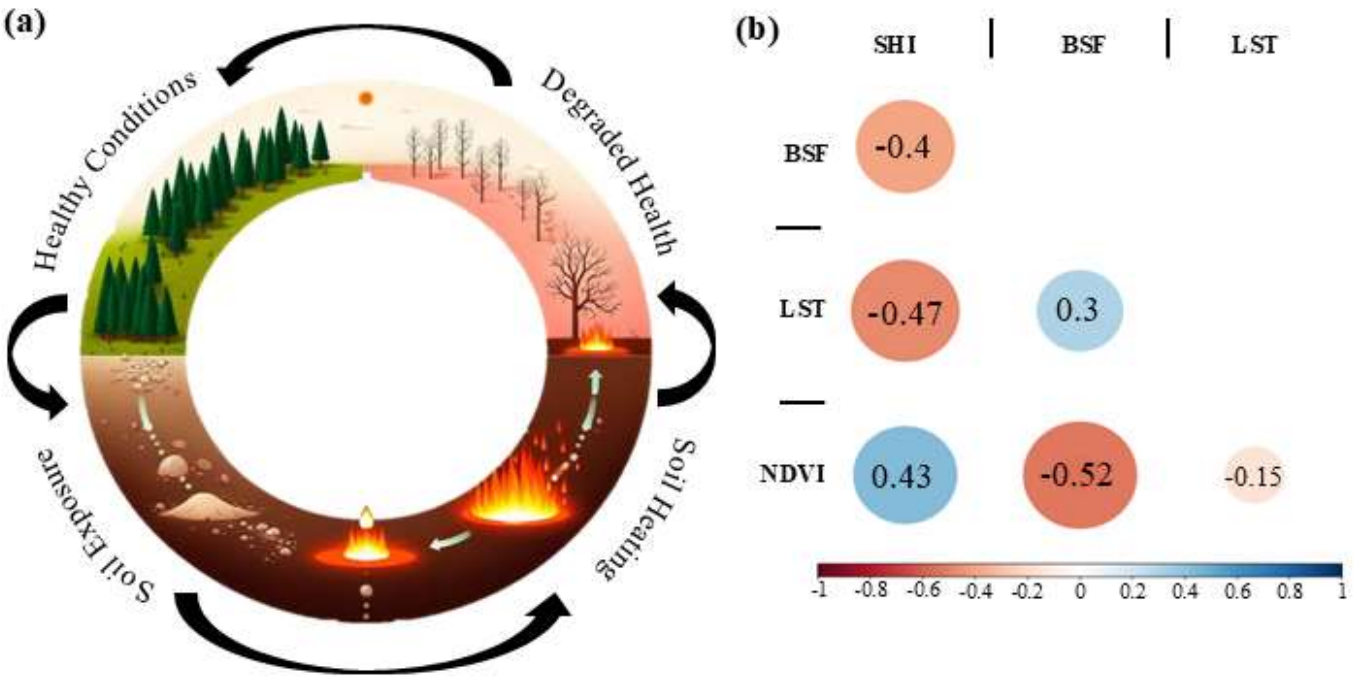

Figure 9. (**a**) Soil degradation processes and (**b**) Correlations between BSF, LST and NDVI.

The BSF reflects the proportion of soil that remains uncovered over time, indicating the level of soil exposure to environmental factors such as rain, wind, and solar radiation [32]. In areas where the soil remains uncovered for extended periods, accelerated degradation processes are observed, including reduced SOC, increased soil compaction, and nutrient loss due to erosion. In this context, CTS, which involves intensive soil disturbance, tends to increase the BSF, resulting in greater vulnerability of the soil to these destructive processes [85].

Bare soils tend to heat up more rapidly, raising surface temperatures, which can negatively impact biological and physicochemical processes in the soil, such as microbial activity crucial for nutrient cycling [86]. Areas with high BSF values often exhibit increased LST due to the lack of vegetation cover, which disrupts the thermal regulation provided by plants [87]. In agreement with our findings (Figure 9b), Song et al. (2018) [88] conducted a global study contrasting LST and NDVI, identifying strong trends of soil warming linked

to decreased vegetation cover. Similarly, our results reveal a direct correlation between the increase in BSF, the reduction in NDVI, and the rise in LST, emphasizing the critical role of vegetation in regulating soil temperature and maintaining SH.

In Figure 9b, it is observed that the BSF has a moderate negative correlation with the SHI ($R = -0.4$, p-value < 0.001), indicating that prolonged bare soil is associated with worsening SH conditions. The positive correlation between BSF and LST ($R = 0.3$, p-value < 0.001) reinforces the idea that soil exposure also contributes to increased surface temperature, intensifying the negative impacts on the soil. These results agree with [49]. These authors conducted a comparative degradation analysis between Brazilian states based on parameters such as BSF, LST, and SOC, identifying management strategies and soils vulnerable to degradation.

The potential of BSF as an analysis factor in soil management is particularly important when compared to no-till farming. No-till farming, which involves maintaining permanent vegetation cover or crop residues on the soil surface, tends to drastically reduce BSF, protecting the soil from erosion, improving water infiltration, and maintaining cooler surface temperatures [89]. Thus, no-till farming contributes to the preservation of SH, whereas conventional tillage, by increasing BSF, exacerbates degradation processes, making it a critical metric for evaluating management practices.

4.3. Geological and Pedological Influences on SH Dynamics in Agricultural Landscapes

To better understand the SH dynamics, we cross-reference data with SHI, geology, and pedology (Figure 7). The two most prevalent soil types in Germany—those derived from sandy layers and Loess or its derivatives—originate from distinct geological formations, which directly influence their natural fertility and resilience. Soils derived from sandy layers are nutrient-poor due to their predominance of sand particles, which offer limited capacity for retaining water and essential nutrients [90]. This inherent limitation often necessitates intensive chemical management practices, such as fertilizer application, to sustain agricultural productivity [91]. Such interventions appear to compensate for the poor nutrient profile, leading to an observed increase in SHI values within these areas. The relatively lower proportion of agricultural land compared to natural or forested areas further supports this, indicating a reliance on targeted management to enhance SH in these zones [92].

Conversely, soils derived from Loess and its derivatives are naturally fertile due to their fine silt particles mixed with small amounts of sand and clay, allowing better water retention and nutrient availability. This inherent fertility makes these soils highly attractive for agricultural expansion, resulting in a higher proportion of agricultural land in such regions [93]. However, unlike the sandy soils, where management is focused on nutrient supplementation, Loess soils often face more extractive farming practices. The natural fertility invites intensive cultivation, which can, over time, lead to soil degradation if sustainable practices are not implemented [94]. This contrast in the relationship between SHI values and agricultural expansion underscores the need for careful management in these fertile areas to maintain their productivity in the long term.

In the context of pedology, Cambisols and Luvisols emerge as the dominant soil classes in Germany [26]. Luvisols, with their favorable texture and nutrient profile, are highly productive and, therefore, are more commonly utilized for agriculture [95]. The marked differences in SHI values between agricultural and forested Luvisols suggest that intensive land use has a noticeable impact on SH in these regions. The productive potential of Luvisols attracts intensive farming, which can diminish soil quality without proper management practices, highlighting the delicate balance between maximizing agricultural output and maintaining soil sustainability [96].

Compared to Luvisols, Cambisols present a different narrative. Cambisols have limited natural fertility and demonstrate a balanced distribution between AGSO and FSO. This balance suggests that Cambisols are often used for mixed land uses that combine forest management with moderate agricultural activities, which can be sustainably managed without severely compromising SH [97]. The relatively stable SHI averages in these areas indicate a more harmonious relationship between anthropogenic activities and natural soil characteristics, contrasting with the more intensive use of Luvisols.

Although the SHI is based on surface attributes (0–20 cm), many of the physical and chemical properties captured at this depth—such as texture, bulk density, pH, and organic matter—are strongly inherited from deeper pedogenetic processes and parent material [98]. This inheritance helps explain why SHI patterns remain coherent when stratified by geological formations and WRB soil groups. Nonetheless, the shallow depth of assessment introduces limitations, as SH responses related to subsoil constraints, deeper horizon development, or long-term pedogenic features may not be fully captured by surface-derived indicators [99].

Thus, while SHI provides a meaningful representation of soil functioning at the surface, its interpretation must consider both the inherited pedological context and the potential mismatch between surface conditions and deeper soil processes. Recognizing this limitation is essential for distinguishing management-driven changes from natural soil variability and for ensuring that SH assessments remain grounded in the broader framework of soil formation.

This nuanced analysis emphasizes the importance of adapting soil management practices to the specific characteristics of each soil type and geological formation. While naturally poor soils like sandy layers may benefit from targeted nutrient interventions, naturally fertile soils such as those derived from Loess require strategies focused on preservation and sustainable extraction to maintain long-term productivity [100]. Similarly, Cambisols and Luvisols present different challenges and opportunities for SH management, underscoring the importance of localized and adaptive strategies that align with both the natural and anthropogenic dynamics influencing SH.

4.4. Economic and Historical Influence on German SH

Figure 10 highlights a positive correlation (R = 0.52) between regional GDP and SHI across German states (Figure 10a). Wealthier regions, such as Baden-Württemberg and Bavaria, exhibit higher SHI values (0.50–0.55), while economically weaker states, particularly in former East Germany (EG), e.g., Brandenburg and Saxony-Anhalt, show lower SHI levels (0.40–0.45). This indicates that economic development can foster improved land management and greater investment in soil-conserving technologies [101–103].

The historical divide between West Germany (WG) and EG strongly influenced current soil conditions. WG, with stronger post-war economic recovery and environmental policies, preserved a larger proportion of forested areas and adopted more sustainable agricultural practices. As shown in Figure 10b, 88% of WG land is classified as having high SHI, whereas 20% of EG area is under low SHI, with 80% considered medium.

The forced intensification of agriculture in EG under socialist governance, combined with limited access to modern technology and less favorable natural conditions (e.g., sandy soils, low precipitation), contributed to widespread soil degradation [104,105]. Additionally, the post-reunification pressure to integrate into a capitalist production system led to unsustainable practices focused on maximizing short-term yields [106,107].

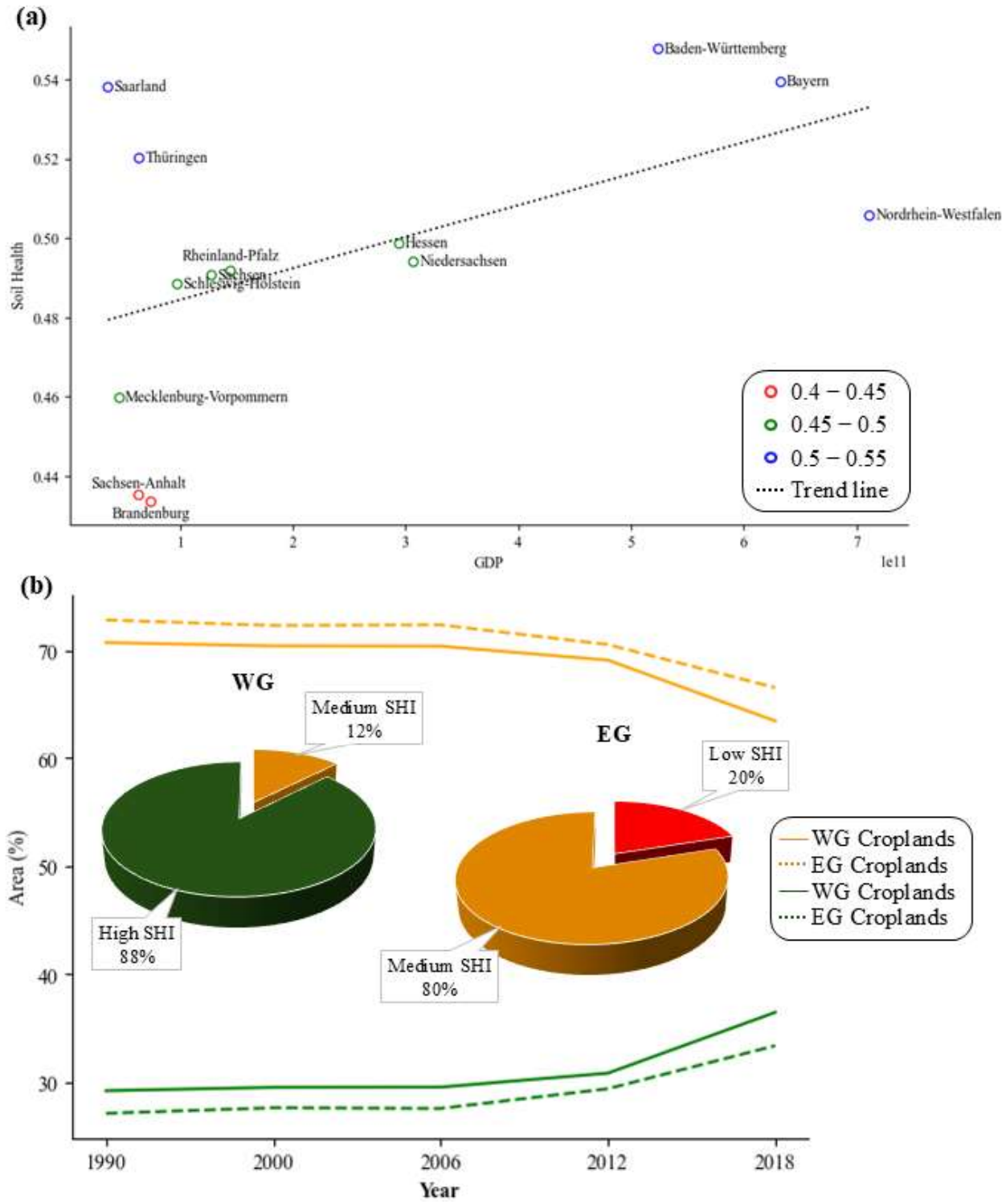

Figure 10. Economic (**a**) and Land use Coverage (**b**) influence on Germany SH.

Despite regional disparities, the findings support the idea that investments in sustainable management return significant long-term benefits. Kirui et al. (2015) [101] estimated that every USD 1 invested in preventing land degradation yields USD 4.3 in returns, while other studies suggest even higher benefits [103]. In summary, the data reinforce that SH is not only shaped by natural conditions but also by socio-economic factors and historical land management decisions. Promoting sustainability requires aligning economic development with effective conservation strategies.

4.5. Interpreting the German SHI in a European SH Context

The German SHI synthesizes national information on key chemical, physical and biological attributes into a single spatially explicit indicator, allowing comparison of soil functioning across contrasting regions. When interpreted alongside recent European initiatives that report more than 60% of EU soils as unhealthy based on multiple degradation indicators, the predominance of moderate SHI values across Germany suggests an intermediate condition: soils are not in a critical state on average, but a large share of the agricultural land base operates below its potential soil-function capacity [108,109]. This aligns with emerging EU-level frameworks that argue for moving beyond a binary "healthy/unhealthy" view towards continuous gradients of soil functioning and risk, where moderate status still warrants targeted management and policy interventions [110,111].

At the same time, the SHI results highlight that national averages can mask strong regional contrasts. Higher SHI values in loess and carbonate soils of southern and central Germany indicate combinations of favorable inherent properties and, in many cases, more diversified or conservation management, whereas lower SHI in sandy northern lowlands and parts of the former East Germany are consistent with lower water- and nutrient-holding capacity and long-term intensification pressures documented in regional assessments [112,113]. These patterns reinforce the notion, widely recognized in recent SH literature, that indicators must be interpreted in the light of soil type, climate and land use history rather than against a single universal threshold [111,114].

Importantly, the SHI integrates only a subset of the indicators currently proposed in European SH dashboards—focusing on topsoil properties and RS drivers such as vegetation cover and soil exposure—while omitting other dimensions such as biodiversity, contaminants and subsoil processes that are now being discussed at EU level [109,115]. As a result, SHI should be viewed as a functional soil-process index tailored to agricultural production and ecosystem-service delivery, not as a full compliance metric for the forthcoming EU Soil Monitoring Law. This partial coverage is a limitation, but it also makes the index operational from existing databases and provides a scalable template that can be progressively enriched as new harmonized indicators (e.g., microbial diversity, biological structure, additional degradation metrics) become available [47,116].

4.6. Strengths, Limitations, and Interpretative Value of SADI

The SADI synthesizes three fundamental dimensions of agricultural sustainability—SH, management intensity, and economic performance—into a single composite indicator. This multidimensional structure provides a powerful interpretative lens for evaluating agricultural systems that extend beyond biophysical constraints alone. However, as with any aggregated index, its interpretative value is shaped by both its conceptual strengths and inherent methodological limitations.

4.6.1. Strengths of the SADI as an Integrative Sustainability Indicator

A principal strength of the SADI lies in its ability to incorporate soil functioning (via SHI), land-management quality (via BSF), and economic viability (via EcF) into a unified analytical framework. This design aligns with the increasing consensus that agricultural sustainability must be evaluated through cross-cutting interactions among ecological, socioeconomic, and management drivers [117]. In this context, the SADI responds to calls for integrative indicators capable of supporting policy, land use planning, and cross-regional benchmarking.

The index also benefits from the robustness of its independent components. SHI is validated through multiple methodological layers, providing a biophysically grounded foundation for the SADI. Similarly, BSF is supported by extensive literature confirming its

role as a proxy for land-management pressure and erosion vulnerability [49,83]. Economic profitability per hectare, derived from official agricultural statistics, introduces an objective and externally verifiable socioeconomic pillar, avoiding model-based circularity.

Furthermore, the SADI captures historically persistent structural differences between German states. Regions with long-standing economic strength—such as Baden-Württemberg or Bavaria—systematically exhibit higher SADI values, reflecting cumulative investments in agricultural modernization, conservation practices, and technological adoption. Conversely, the lower SADI values in former East German states mirror well-documented legacies of socialist land consolidation, mechanized intensification, and post-reunification production pressures [118,119]. This convergence between the SADI and well-established political–economic trajectories underscores the index's interpretative coherence.

4.6.2. Methodological and Conceptual Limitations

Despite its integrative strengths, the SADI exhibits several key limitations that must be explicitly considered when interpreting its outputs. First, the index inherits spatial uncertainty from its SHI component. While some soil attributes (e.g., pH, BD) demonstrate low uncertainty, others—such as P, K, SOC, and CEC—exhibit moderate to high uncertainty in northern and central transitional landscapes. These propagated uncertainties can attenuate the reliability of SADI values in specific regions, especially where SHI exerts a strong influence due to its weight in the index.

Second, BSF, while a powerful indicator of soil exposure and management intensity, does not fully capture the spectrum of management practices relevant to sustainability—such as crop rotations, residue retention, biological inputs, or precision fertilization. In regions where soil cover is maintained artificially (e.g., winter cover crops, mulching), BSF alone may underestimate degradation risks, whereas in highly heterogeneous crop mosaics it may overestimate them. This type of management ambiguity has been highlighted in recent critiques of RS-derived degradation proxies [83,120].

Third, the economic factor introduces a structural asymmetry into the index, where profitability fluctuates not only with management efficiency but also with market volatility, subsidy allocation, crop-type specialization, and commodity cycles. As a result, regions with inherently unfavorable soils may still obtain artificially high SADI values if supported by strong market mechanisms, while areas with high soil functioning may appear comparatively weaker if dependent on low-value crops, an inherent tension in mixed biophysical and economic indices.

Fourth, the weighting scheme (0.5 for SHI, 0.3 for BSF, 0.2 for EcF) embeds normative assumptions about the relative importance of ecological versus economic criteria. Although the scheme is explicitly justified, it remains a conceptual choice rather than an empirically optimized structure, similar to limitations identified in other sustainability indices [121]. Alternative weighting strategies, such as equal weights, data-driven weights, or region-specific weights, would necessarily yield different SADI spatial patterns.

4.6.3. Interpreting the SADI in the Context of German Agricultural Landscapes

The interpretative value of the SADI is substantial, but its outputs must be contextualized within regional pedology, management systems, and socioeconomic structures. High SADI values do not imply uniformly sustainable soils; rather, they indicate territories where soil functioning, management cover, and economic performance converge positively. Conversely, low SADI values reflect multidimensional vulnerability, not just poor soil conditions.

Importantly, the functional equilibrium analysis reveals that the three SHI functions (biological, physical, and chemical) increase in magnitude across SADI classes but retain nearly constant balance. This indicates that the SADI is more sensitive to the absolute level of soil functioning than to functional symmetry. In other words, the SADI captures how much soil functions are expressed but not how evenly they are expressed—an interpretative nuance that should guide its use in sustainability assessments.

Finally, the SADI should be viewed as a mid-scale policy indicator rather than a fine-scale decision-support tool. It is exceptionally useful for: (i) benchmarking states; (ii) identifying structural disparities; (iii) guiding national investment strategies; (iv) supporting EU-level monitoring frameworks. However, due to uncertainty propagation, management ambiguity, and economic asymmetries, it is not suitable for farm-level recommendations without complementary local data.

4.6.4. Empirical Demonstration of SADI Interpretability: A Contrast Between Rheinland-Pfalz and Sachsen-Anhalt

To illustrate the practical interpretative value of the SADI, we conducted a comparative assessment between two German states with historically contrasting agricultural, socioeconomic, and management contexts: Rheinland-Pfalz (high SADI) and Sachsen-Anhalt (low SADI). Figure 11 integrates the three pillars of the SADI—management (MnF), environmental soil functioning (EnF), and economic performance (EcF)—together with land use structure, enabling a multidimensional interpretation of the factors shaping each state's sustainability profile.

Rheinland-Pfalz exhibits substantially lower BSF (MnF = 6.46%), reflecting reduced soil exposure and higher adoption of conservation practices. Its mean SHI value (EnF = 0.51) is also comparatively higher, indicating better soil functioning and lower degradation pressure. Economically, Rheinland-Pfalz shows a profitability of 1.072 € ha^{-1}, supported by diversified land use, including vineyards (8%), which contribute to high-value production systems and regional economic resilience. The state's land use mosaic—balanced between pastures, croplands, and perennial systems—aligns with the SADI's assumption that multifunctional landscapes tend to support more sustainable management outcomes.

In contrast, Sachsen-Anhalt presents a markedly different sustainability configuration. The state shows a MnF of 17.03%, nearly three times higher than Rheinland-Pfalz, reflecting widespread soil exposure associated with large-scale mechanized systems and historical reliance on extensive cereal monocultures. The EnF value (SHI = 0.44) indicates poorer soil functioning, consistent with long-standing documentation of degradation patterns across the northern and eastern lowlands. Economically, Sachsen-Anhalt's profitability (285 € ha^{-1}) is substantially lower, driven by crop systems with modest market returns and limited diversification. Its land use is overwhelmingly dominated by non-irrigated arable land (83%), reflecting structural legacies of socialist-era land consolidation and reduced economic buffering capacity.

Together, these contrasts demonstrate that the SADI does not simply map soil quality or economic strength in isolation; rather, it captures how soil functioning, management pressure, and economic performance co-vary across space. Importantly, the decomposition of each SADI pillar reveals that low values emerge from different combinations of limiting factors—in Sachsen-Anhalt, soil degradation and management intensity play the dominant role, whereas in Rheinland-Pfalz the higher SADI stems from the combined effect of better soil conditions, diversified land use, and stronger economic performance.

This case study also exposes structural limitations of the index. The relatively high weight of SHI means that areas with strong economic performance but weak soils may still obtain moderate SADI values, while regions with high soil quality but low-value cropping systems risk being penalized. Nevertheless, the comparative assessment confirms that the

SADI is effective in capturing historically persistent regional disparities, reflecting both pedological constraints and long-term socioeconomic trajectories.

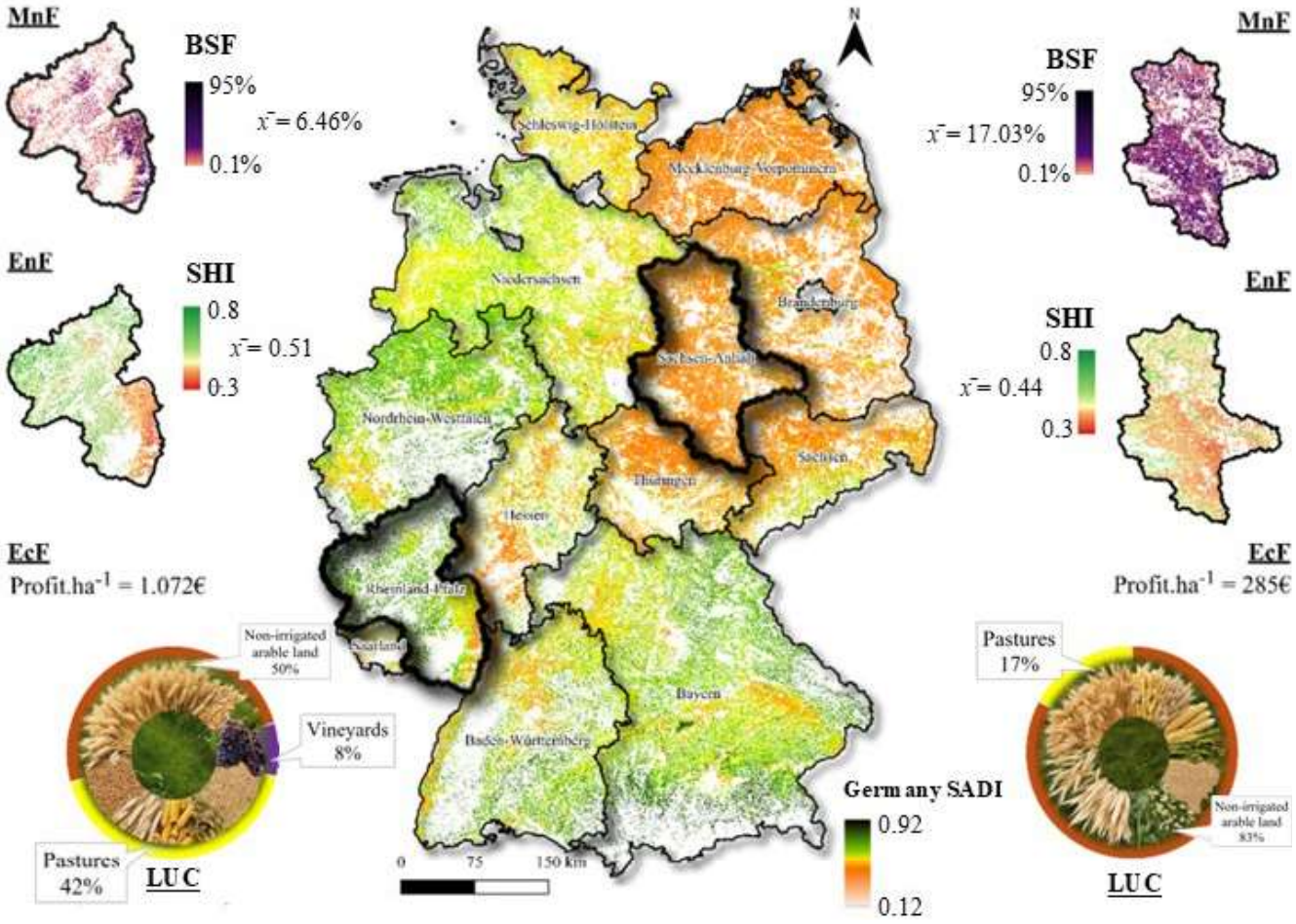

Figure 11. Map of the German SADI.

Overall, the Rheinland-Pfalz vs. Sachsen-Anhalt comparison demonstrates that the SADI provides a coherent, interpretable, and multidimensional representation of agricultural sustainability, while simultaneously exposing the need for context-aware interpretation—particularly in regions shaped by contrasting historical, economic, and land use legacies.

4.7. Methodological Limitations, Data Gaps, and Future Directions for SH and Sustainability Monitoring in Germany

Despite the methodological advances achieved by integrating soil functions, RS indicators, and socioeconomic metrics into the SHI and SADI frameworks, the results highlight several structural limitations that constrain the precision, interpretative power, and policy relevance of national-scale soil-health assessments in Germany. These limitations emerge from gaps in input data, model uncertainty, spatial heterogeneity, and conceptual assumptions embedded within the indices. Addressing them will be central for developing a next-generation soil-monitoring system capable of supporting long-term agricultural sustainability under climate, economic, and land use pressures.

4.7.1. Structural Limitations in Soil Data and Digital Soil Mapping Approaches

The efficient sampling strategies constitute a major structural limitation in DSM [21]. Historically, the recording of sample analysis dates has not been performed systematically,

which hinders any robust assessment of temporal changes in soil parameters. Although recent efforts have improved awareness of the importance of timestamping soil observations, available datasets remain heterogeneous, sparse, and largely lacking consistent temporal information [22]. As a result, it becomes unfeasible to properly model the temporal variation in soil attributes. Therefore, we acknowledge the limitation of representing the current state of soil parameters in a generalized manner, generating modeled values for a fixed point in time without fully capturing their temporal dynamics. Such limitations mirror challenges documented in European-scale DSM efforts, where sandy parent materials and heterogeneous anthropogenic inputs consistently degrade model performance [122]. As a result, national soil-function maps, while informative at broad scales, must be interpreted cautiously when used for local or sub-regional planning.

Remote-sensing proxies add a second layer of constraints. While BSF and NDVI provide valuable ecological signals, they remain partly insensitive to management nuances such as multi-year rotations, residue strategies, or organic amendments. This introduces ambiguity when interpreting management effects solely through satellite-derived indices. Prior studies have warned that RS-based degradation indicators tend to oversimplify complex agroecosystem processes, particularly in temperate cropping systems with high seasonal dynamism [16].

Moreover, the composite nature of SHI, aggregating chemical, physical, and biological proxies, means that uncertainty propagates across soil functions in non-linear ways. The relatively stable functional balance across SADI classes (SD $\approx$ 0.10) (Figure 8) suggests that although soils improve in absolute function, their internal symmetry remains constant; however, this also implies that the SHI may be underrepresenting true multifunctionality deficits in highly managed or structurally degraded systems.

4.7.2. Conceptual and Interpretative Constraints of Composite Sustainability Indices

The SADI introduces additional conceptual limitations. Its weighting structure (0.5 SHI, 0.3 BSF, 0.2 EcF), although transparent, embeds normative assumptions about the relative importance of ecological versus economic sustainability. Alternative weighting schemes—data-driven, region-specific, or expert-derived—would yield different rankings and potentially alter policy priorities. Similar concerns have been raised regarding composite sustainability indices globally, which often inherit implicit value judgments that influence policy outcomes [121].

The EcF also introduces volatility and exogenous noise into the index. Profitability reflects market cycles, subsidy schemes, crop portfolios, and global price shocks, not only intrinsic sustainability. This creates asymmetries: soils with high SHI may appear "less sustainable" under low-value commodity systems, while soils with significant biophysical degradation may be masked by high economic returns—as previously observed in European intensification zones [123].

Similarly, the reliance on SHI functional magnitude rather than functional balance means that soils with high but uneven contributions (e.g., chemically strong but biologically weak) may be misinterpreted as fully healthy. This issue underscores a broader challenge in soil-function mapping: ecosystem functionality is multi-dimensional and cannot be fully captured by aggregating standardized scores.

4.8. Key Data Gaps Limiting National SH Monitoring

4.8.1. Biological Soil Indicators Remain Underrepresented

Although microbial processes are central to soil functioning, national datasets for microbial biomass, enzymatic activity, respiration, or DNA-based metrics are sparse. This

gap limits the ecological resolution of the SHI. Recent calls for integrating biological soil monitoring into EU programs emphasize this deficiency [5].

4.8.2. High-Resolution, Management-Explicit Data Are Largely Absent

Germany lacks harmonized national repositories describing tillage intensity, residue retention, organic amendments, or cover-cropping adoption. Without this information, management-related degradation cannot be reliably mapped.

4.8.3. Temporal Monitoring Remains Insufficient

SHI and SADI represent static snapshots, whereas sustainable agricultural development is inherently dynamic. Climate change, market pressures, and land use conversion require annual—or even intra-annual—tracking systems, as already implemented for LUCAS Soil in pilot temporal expansions [124].

4.8.4. Future Directions

Addressing the limitations identified in the current SHI and SADI frameworks will require coordinated methodological, institutional, and technological advances capable of strengthening the national soil-monitoring infrastructure. A first priority is the establishment of periodic national re-sampling campaigns, particularly in northern sandy regions and intensively cultivated belts, where our uncertainty analysis showed the greatest prediction errors for P, K, CEC and SOC. Increasing sample density in these structurally heterogeneous landscapes would substantially reduce spatial uncertainty and improve the robustness of soil-function mapping, a limitation repeatedly noted in continental assessments such as [122,125].

A second methodological direction is the systematic integration of proximal sensing technologies. Portable mid-infrared (MIR) spectroscopy, X-ray fluorescence (XRF), and related in-field spectroscopic tools offer rapid, cost-efficient acquisition of high-quality soil spectral data, enabling large-scale model refinement at substantially lower cost than traditional laboratory analysis. Their effectiveness has already been demonstrated across Europe [126,127].

Third, Germany lacks harmonized national datasets describing land-management practices, including tillage intensity, cover-cropping, residue retention, and organic amendments. Developing standardized management-layer datasets would directly strengthen the interpretative validity of BSF, SHI and SADI, allowing degradation processes to be linked not only to biophysical patterns but also to specific management regimes. This type of integration has been repeatedly recommended in high-impact reviews on soil sustainability [5].

Fourth, the development of temporal SHI and SADI products, updated annually or seasonally using satellite archives and dynamic modeling, would allow monitoring of degradation, recovery, and management shifts in near-real time. Such temporalization is essential for capturing climate-induced changes, extreme-event responses, and evolving management patterns, none of which are represented in current static products.

Finally, future versions of the SADI would benefit from the incorporation of hybrid risk-based indicators combining economic resilience with ecological thresholds (e.g., drought sensitivity, nutrient-loss potential, or erosion susceptibility). These additions would prevent overemphasis on short-term profitability and align the index more closely with long-term sustainability and resilience objectives, an issue highlighted across the environmental-economics literature.

Taken together, these methodological directions form a coherent roadmap for advancing German SH monitoring into a system that is spatially resolved, management-explicit,

temporally dynamic, and ecologically meaningful—bridging the gap between national sustainability assessments and farm-level decision making.

5. Conclusions

This study provides the first nationally consistent, spatially explicit assessment of SH and sustainable agricultural development in Germany. The SHI revealed that most German soils fall within moderate health conditions, driven by natural pedological constraints in the north and persistent management pressures in the east. While the spatial patterns of key soil attributes align with established geological and pedogenetic gradients, the uncertainty analysis shows that P, K, CEC, and SOC remain unreliable in transitional landscapes, indicating that national soil mapping must be interpreted with caution and supported by targeted resampling efforts.

The SHI showed strong ecological validity when compared with NDVI, BSF, and SOC, confirming its capacity to identify functional differences in soil condition. SADI expanded this perspective by integrating soil functioning, management intensity, and profitability, highlighting structural disparities between western and eastern states. However, its use is constrained by uncertainties propagated from the SHI, by BSF limited representation of management complexity, and by the sensitivity of profitability to market forces rather than long-term sustainability.

Overall, SHI and SADI offer powerful tools for national-scale diagnosis but must be treated as strategic indicators rather than prescriptive decision tools. Advancing their reliability will require denser soil resampling networks, integration of proximal sensing technologies, national datasets on tillage and residue management, and the development of temporal SHI/SADI products capable of tracking yearly degradation and recovery. Incorporating resilience and risk metrics will further strengthen the SADI, ensuring that sustainability assessments reflect long-term ecological stability, not short-term economic outcomes.

Together, these findings demonstrate that Germany's SH and SADI are shaped by the combined influence of soil functions, land management, and historical–economic trajectories, and that future policies must explicitly integrate these dimensions to support a transition toward more resilient agricultural systems.

Author Contributions: G.P.B.d.S.: Writing—review and editing, Writing—original draft, Visualization, Validation, Supervision, Software, Resources, Project administration, Methodology, Investigation, Funding acquisition, Formal analysis, Data curation, Conceptualization. J.A.M.D.: Writing—review and editing, Writing—original draft, Visualization, Validation, Supervision, Software, Resources, Project administration, Methodology, Investigation, Funding acquisition, Formal analysis, Data curation, Conceptualization. S.C.: Writing—review and editing, Visualization, Validation, Resources. R.M.: Writing—review and editing, Visualization, Validation. R.R.P.: Data availability. M.T.A.A.: Writing—review and editing. B.d.A.B.: Writing—review and editing. J.T.F.R.: Writing—review and editing. M.R.C.: Writing—review and editing, Methodology. Y.M.: Writing—review and editing. R.B.d.O.: Writing—review and editing, M.R.N.: Writing—review and editing, R.F.: Writing—review and editing. All authors have read and agreed to the published version of the manuscript.

Funding: This research was funded by FAPESP, grant number 2025/02264-2; 2021/05129-8; 2021/10573-4.

Data Availability Statement: The data presented in this study are available on request from the corresponding author due to privacy information.

Conflicts of Interest: The authors declare no conflicts of interest.

Abbreviations

The following abbreviations are used in this manuscript:

SH	Soil Health
SHI	Soil Health Index
RS	Remote Sensing
ML	Machine Learning
BSO	Surrounding Points
SOM	Soil Organic Matter
SADI	Sustainable Agricultural Development Index
ANSO	Anthropogenic Areas
AGSO	Agricultural Areas
FSO	Forest Areas
BD	Bulk Density
SOC	Soil Organic Carbon
K	Potassium
N	Nitrogen
CEC	Cation-exchange Capacity
P	Phosphorus
GEOS3	Geospatial Soil Sensing System
SYSI	Synthetic Soil Image
DEM	Digital Elevation Model
MAT	Mean Annual Temperature
AP	Annual Precipitation
TAR	Temperature Annual Range
OS	Seasonal Precipitation
LST	Land Surface Temperature
GEE	Google Earth Engine
MIB	More is Better
LIB	Less is Better
OMI	Optimal Midpoint
NDVI	Normalized Difference Vegetation Index
BSF	Bare Soil Frequency
EcF	Economic Factor
EnF	Environmental Factor
MnF	Management Factor
CTS	Conventional Tillage Systems
WG	West Germany
EG	East Germany
DSM	Digital Soil Mapping

References

1. Smith, P.; Poch, R.M.; Lobb, D.A.; Bhattacharyya, R.; Alloush, G.; Eudoxie, G.D.; Anjos, L.H.C.; Castellano, M.; Ndzana, G.M.; Chenu, C.; et al. Status of the World's Soils. *Annu. Rev. Environ. Resour.* **2024**, *49*, 73–104. [CrossRef]
2. Chure, G.; Banks, R.A.; Flamholz, A.I.; Sarai, N.S.; Kamb, M.; Lopez-Gomez, I.; Bar-On, Y.M.; Milo, R.; Phillips, R. The Anthropocene by the Numbers: A Quantitative Snapshot of Humanity's Influence on the Planet. *arXiv* **2021**, arXiv:2101.09620.
3. Molotoks, A.; Smith, P.; Dawson, T.P. Impacts of Land Use, Population, and Climate Change on Global Food Security. *Food Energy Secur.* **2021**, *10*, e261. [CrossRef]
4. Falcon, W.P.; Naylor, R.L.; Shankar, N.D. Rethinking Global Food Demand for 2050. *Popul. Dev. Rev.* **2022**, *48*, 921–957. [CrossRef]
5. Lehmann, J.; Bossio, D.A.; Kögel-Knabner, I.; Rillig, M.C. The Concept and Future Prospects of Soil Health. *Nat. Rev. Earth Environ.* **2020**, *1*, 544–553. [CrossRef]
6. Yang, T.; Siddique, K.H.M.; Liu, K. Cropping Systems in Agriculture and Their Impact on Soil Health-A Review. *Glob. Ecol. Conserv.* **2020**, *23*, e01118. [CrossRef]

7. Bünemann, E.K.; Bongiorno, G.; Bai, Z.; Creamer, R.E.; De Deyn, G.; de Goede, R.; Fleskens, L.; Geissen, V.; Kuyper, T.W.; Mäder, P.; et al. Soil Quality—A Critical Review. *Soil Biol. Biochem.* **2018**, *120*, 105–125. [CrossRef]
8. Doran, J.W.; Coleman, D.C.; Bezdicek, D.F.; Stewart, B.A. Defining Soil Quality for a Sustainable Environment. In *Defining Soil Quality for a Sustainable Environment*; Soil Science Society of America: Madison, WI, USA, 2015; pp. 1–244. [CrossRef]
9. Stevens, A.W. Review: The Economics of Soil Health. *Food Policy* **2018**, *80*, 1–9. [CrossRef]
10. Bouma, J.; Bonfante, A.; Basile, A.; van Tol, J.; Hack-ten Broeke, M.J.D.; Mulder, M.; Heinen, M.; Rossiter, D.G.; Poggio, L.; Hirmas, D.R. How Can Pedology and Soil Classification Contribute towards Sustainable Development as a Data Source and Information Carrier? *Geoderma* **2022**, *424*, 115988. [CrossRef]
11. Norfleet, M.L.; Ditzler, C.A.; Puckett, W.E.; Grossman, R.B.; Shaw, J.N. Soil quality and its relationship to pedology. *Soil Sci.* **2003**, *168*, 149–155. [CrossRef]
12. Juhos, K.; Szabó, S.; Ladányi, M. Explore the Influence of Soil Quality on Crop Yield Using Statistically-Derived Pedological Indicators. *Ecol. Indic.* **2016**, *63*, 366–373. [CrossRef]
13. Fausak, L.K.; Bridson, N.; Diaz-Osorio, F.; Jassal, R.S.; Lavkulich, L.M. Soil Health—A Perspective. *Front. Soil Sci.* **2024**, *4*, 1462428. [CrossRef]
14. Bonfante, A.; Terribile, F.; Bouma, J. Refining Physical Aspects of Soil Quality and Soil Health When Exploring the Effects of Soil Degradation and Climate Change on Biomass Production: An Italian Case Study. *Soil* **2019**, *5*, 1–14. [CrossRef]
15. Grunwald, S.; Vasques, G.M.; Rivero, R.G. Fusion of Soil and Remote Sensing Data to Model Soil Properties. *Adv. Agron.* **2015**, *131*, 1–109. [CrossRef]
16. Wang, J.; Zhen, J.; Hu, W.; Chen, S.; Lizaga, I.; Zeraatpisheh, M.; Yang, X. Remote Sensing of Soil Degradation: Progress and Perspective. *Int. Soil Water Conserv. Res.* **2023**, *11*, 429–454. [CrossRef]
17. Poppiel, R.R.; Cherubin, M.R.; Novais, J.J.M.; Demattê, J.A.M. Soil Health in Latin America and the Caribbean. *Commun. Earth Environ.* **2025**, *6*, 141. [CrossRef]
18. Tripathi, A.; Tiwari, R.K.; Tiwari, S.P. A Deep Learning Multi-Layer Perceptron and Remote Sensing Approach for Soil Health Based Crop Yield Estimation. *Int. J. Appl. Earth Obs. Geoinf.* **2022**, *113*, 102959. [CrossRef]
19. Khosravi Aqdam, K.; Rezapour, S.; Asadzadeh, F.; Nouri, A. An Integrated Approach for Estimating Soil Health: Incorporating Digital Elevation Models and Remote Sensing of Vegetation. *Comput. Electron. Agric.* **2023**, *210*, 107922. [CrossRef]
20. Savin, I.Y.; Zhogolev, A.V.; Prudnikova, E.Y. Modern Trends and Problems of Soil Mapping. *Eurasian Soil Sci.* **2019**, *52*, 471–480. [CrossRef]
21. Huang, H.; Yang, L.; Zhang, L.; Pu, Y.; Yang, C.; Wu, Q.; Cai, Y.; Shen, F.; Zhou, C. A Review on Digital Mapping of Soil Carbon in Cropland: Progress, Challenge, and Prospect. *Environ. Res. Lett.* **2022**, *17*, 123004. [CrossRef]
22. Piikki, K.; Wetterlind, J.; Söderström, M.; Stenberg, B. Perspectives on Validation in Digital Soil Mapping of Continuous Attributes—A Review. *Soil Use Manag.* **2021**, *37*, 7–21. [CrossRef]
23. Sklenicka, P.; Zouhar, J.; Molnarova, K.J.; Vlasak, J.; Kottova, B.; Petrzelka, P.; Gebhart, M.; Walmsley, A. Trends of Soil Degradation: Does the Socio-Economic Status of Land Owners and Land Users Matter? *Land Use Policy* **2020**, *95*, 103992. [CrossRef]
24. Zambon, I.; Benedetti, A.; Ferrara, C.; Salvati, L. Soil Matters? A Multivariate Analysis of Socioeconomic Constraints to Urban Expansion in Mediterranean Europe. *Ecol. Econ.* **2018**, *146*, 173–183. [CrossRef]
25. Peel, M.C.; Finlayson, B.L.; Mcmahon, T.A. Updated World Map of the Koppen-Geiger Climate Classification. *Hydrol. Earth Syst. Sci.* **2007**, *11*, 1633–1644. [CrossRef]
26. BGR Soil Map of the Federal Republic of Germany 1:1,000,000. Available online: https://inspire-geoportal.ec.europa.eu/srv/api/records/A95A723E-1274-4601-9E60-27079436F1F3 (accessed on 1 May 2024).
27. BGR Geoportal Gruppen Der Bodenausgangsgesteine in Deutschland 1:5,000,000. Available online: https://geoportal.bgr.de/mapapps/resources/apps/geoportal/index.html?lang=de#/datasets/portal/30D75B66-DB78-4298-B80F-B7AFBD798DAE (accessed on 4 July 2024).
28. CORINE Land Cover 2018 (Raster 100 m), Europe, 6-Yearly—Version 2020_20u1. 2020. Available online: https://sdi.eea.europa.eu/catalogue/copernicus/api/records/960998c1-1870-4e82-8051-6485205ebbac?language=all (accessed on 31 July 2024).
29. McBratney, A.B.; Mendonça Santos, M.L.; Minasny, B. On Digital Soil Mapping. *Geoderma* **2003**, *117*, 3–52. [CrossRef]
30. Hijmans, R.J.; Cameron, S.E.; Parra, J.L.; Jones, P.G.; Jarvis, A. Very High Resolution Interpolated Climate Surfaces for Global Land Areas. *Int. J. Climatol.* **2005**, *25*, 1965–1978. [CrossRef]
31. Safanelli, J.L.; Poppiel, R.R.; Chimelo Ruiz, L.F.; Bonfatti, B.R.; de Oliveira Mello, F.A.; Rizzo, R.; Demattê, J.A.M. Terrain Analysis in Google Earth Engine: A Method Adapted for High-Performance Global-Scale Analysis. *ISPRS Int. J. Geoinf.* **2020**, *9*, 400. [CrossRef]
32. Demattê, J.A.M.; Fongaro, C.T.; Rizzo, R.; Safanelli, J.L. Geospatial Soil Sensing System (GEOS3): A Powerful Data Mining Procedure to Retrieve Soil Spectral Reflectance from Satellite Images. *Remote Sens Environ.* **2018**, *212*, 161–175. [CrossRef]
33. Ermida, S.L.; Soares, P.; Mantas, V.; Göttsche, F.M.; Trigo, I.F. Google Earth Engine Open-Source Code for Land Surface Temperature Estimation from the Landsat Series. *Remote Sens.* **2020**, *12*, 1471. [CrossRef]

34. Carvalho Mendes, I.; Martinhão Gomes Sousa, D.; Dario Dantas, O.; Alves Castro Lopes, A.; Bueno Reis Junior, F.; Ines Oliveira, M.; Montandon Chaer, G. Soil Quality and Grain Yield: A Win–Win Combination in Clayey Tropical Oxisols. *Geoderma* **2021**, *388*, 114880. [CrossRef]
35. Silvero, N.E.Q.; Demattê, J.A.M.; Amorim, M.T.A.; dos Santos, N.V.; Rizzo, R.; Safanelli, J.L.; Poppiel, R.R.; de Sousa Mendes, W.; Bonfatti, B.R. Soil Variability and Quantification Based on Sentinel-2 and Landsat-8 Bare Soil Images: A Comparison. *Remote Sens. Environ.* **2021**, *252*, 112117. [CrossRef]
36. Rosas, J.T.F.; Demattê, J.A.M.; Rosin, N.A.; dos Anjos Bartsch, B.; Poppiel, R.R.; Rodriguez-Albarracin, H.S.; Novais, J.J.M.; Pavinato, P.S.; Ma, Y.; Mello, D.C.D.; et al. Geotechnologies on the Phosphorus Stocks Determination in Tropical Soils: General Impacts on Society. *Sci. Total Environ.* **2024**, *938*, 173537. [CrossRef] [PubMed]
37. Cherubin, M.R.; Karlen, D.L.; Cerri, C.E.P.; Franco, A.L.C.; Tormena, C.A.; Davies, C.A.; Cerri, C.C. Soil Quality Indexing Strategies for Evaluating Sugarcane Expansion in Brazil. *PLoS ONE* **2016**, *11*, e0150860. [CrossRef] [PubMed]
38. Rinot, O.; Levy, G.J.; Steinberger, Y.; Svoray, T.; Eshel, G. Soil Health Assessment: A Critical Review of Current Methodologies and a Proposed New Approach. *Sci. Total Environ.* **2019**, *648*, 1484–1491. [CrossRef]
39. Chang, T.; Feng, G.; Paul, V.; Adeli, A.; Brooks, J.P. Soil Health Assessment Methods: Progress, Applications and Comparison. *Adv. Agron.* **2022**, *172*, 129–210. [CrossRef]
40. Phillips, H.R.P.; Bach, E.M.; Bartz, M.L.C.; Bennett, J.M.; Beugnon, R.; Briones, M.J.I.; Brown, G.G.; Ferlian, O.; Gongalsky, K.B.; Guerra, C.A.; et al. Global Data on Earthworm Abundance, Biomass, Diversity and Corresponding Environmental Properties. *Sci. Data* **2021**, *8*, 136. [CrossRef]
41. Piron, D.; Boizard, H.; Heddadj, D.; Pérès, G.; Hallaire, V.; Cluzeau, D. Indicators of Earthworm Bioturbation to Improve Visual Assessment of Soil Structure. *Soil Tillage Res.* **2017**, *173*, 53–63. [CrossRef]
42. Adhikari, K.; Hartemink, A.E. Linking Soils to Ecosystem Services—A Global Review. *Geoderma* **2016**, *262*, 101–111. [CrossRef]
43. Drobnik, T.; Greiner, L.; Keller, A.; Grêt-Regamey, A. Soil Quality Indicators—From Soil Functions to Ecosystem Services. *Ecol. Indic.* **2018**, *94*, 151–169. [CrossRef]
44. Lima, A.C.R.; Brussaard, L.; Totola, M.R.; Hoogmoed, W.B.; de Goede, R.G.M. A Functional Evaluation of Three Indicator Sets for Assessing Soil Quality. *Appl. Soil Ecol.* **2013**, *64*, 194–200. [CrossRef]
45. Oldoni, H.; Tavares, T.R.; Brasco, T.L.; Cherubin, M.R.; de Carvalho, H.W.P.; Magalhães, P.S.G.; do Amaral, L.R. Temporal Evaluation of Soil Chemical Quality Using VNIR and XRF Spectroscopies. *Soil Tillage Res.* **2024**, *240*, 106087. [CrossRef]
46. Prăvălie, R.; Borrelli, P.; Panagos, P.; Ballabio, C.; Lugato, E.; Chappell, A.; Miguez-Macho, G.; Maggi, F.; Peng, J.; Niculiță, M.; et al. A Unifying Modelling of Multiple Land Degradation Pathways in Europe. *Nat. Commun.* **2024**, *15*, 3862. [CrossRef] [PubMed]
47. Panagos, P.; Broothaerts, N.; Ballabio, C.; Orgiazzi, A.; De Rosa, D.; Borrelli, P.; Liakos, L.; Vieira, D.; Van Eynde, E.; Arias Navarro, C.; et al. How the EU Soil Observatory Is Providing Solid Science for Healthy Soils. *Eur. J. Soil Sci.* **2024**, *75*, e13507. [CrossRef]
48. BMEL—Statistik: Buchführungsergebnisse Landwirtschaft 2021/22. Available online: https://www.bmel-statistik.de/landwirtschaft/testbetriebsnetz/testbetriebsnetz-landwirtschaft-buchfuehrungsergebnisse/archiv-buchfuehrungsergebnisse-landwirtschaft/buchfuehrungsergebnisse-landwirtschaft-2021/22 (accessed on 1 December 2025).
49. De Sousa, G.P.B.; Bellinaso, H.; Rosas, J.T.F.; de Mello, D.C.; Rosin, N.A.; Amorim, M.T.A.; dos Anjos Bartsch, B.; Cardoso, M.C.; Mallah, S.; Francelino, M.R.; et al. Assessing Soil Degradation in Brazilian Agriculture by a Remote Sensing Approach to Monitor Bare Soil Frequency: Impact on Soil Carbon. *Soil Adv.* **2024**, *2*, 100011. [CrossRef]
50. Safanelli, J.L.; Chabrillat, S.; Ben-Dor, E.; Demattê, J.A.M. Multispectral Models from Bare Soil Composites for Mapping Topsoil Properties over Europe. *Remote Sens.* **2020**, *12*, 1369. [CrossRef]
51. Sayão, V.M.; dos Santos, N.V.; de Sousa Mendes, W.; Marques, K.P.P.; Safanelli, J.L.; Poppiel, R.R.; Demattê, J.A.M. Land Use/Land Cover Changes and Bare Soil Surface Temperature Monitoring in Southeast Brazil. *Geoderma Reg.* **2020**, *22*, e00313. [CrossRef]
52. Nascimento, C.M.; Demattê, J.A.M.; Mello, F.A.O.; Rosas, J.T.F.; Tayebi, M.; Bellinaso, H.; Greschuk, L.T.; Albarracín, H.S.R.; Ostovari, Y. Soil Degradation Detected by Temporal Satellite Image in São Paulo State, Brazil. *J. South Am. Earth Sci.* **2022**, *120*, 104036. [CrossRef]
53. Li, J.; Ren, T.; Li, Y.; Chen, N.; Yin, Q.; Li, M.; Liu, H.; Liu, G. Organic Materials with High C/N Ratio: More Beneficial to Soil Improvement and Soil Health. *Biotechnol. Lett.* **2022**, *44*, 1415–1429. [CrossRef]
54. Arthur, E.; Tuller, M.; Moldrup, P.; de Jonge, L.W. Clay Content and Mineralogy, Organic Carbon and Cation Exchange Capacity Affect Water Vapour Sorption Hysteresis of Soil. *Eur. J. Soil Sci.* **2020**, *71*, 204–214. [CrossRef]
55. Chen, H.; Marhan, S.; Billen, N.; Stahr, K. Soil Organic-Carbon and Total Nitrogen Stocks as Affected by Different Land Uses in Baden-Württemberg (Southwest Germany). *J. Plant Nutr. Soil Sci.* **2009**, *172*, 32–42. [CrossRef]
56. Schrumpf, M.; Kaiser, K.; Schulze, E.D. Soil Organic Carbon and Total Nitrogen Gains in an Old Growth Deciduous Forest in Germany. *PLoS ONE* **2014**, *9*, e89364. [CrossRef]
57. Solly, E.F.; Weber, V.; Zimmermann, S.; Walthert, L.; Hagedorn, F.; Schmidt, M.W.I. A Critical Evaluation of the Relationship Between the Effective Cation Exchange Capacity and Soil Organic Carbon Content in Swiss Forest Soils. *Front. For. Glob. Change* **2020**, *3*, 566869. [CrossRef]

58. Yuzugullu, O.; Lorenz, F.; Fröhlich, P.; Liebisch, F. Understanding Fields by Remote Sensing: Soil Zoning and Property Mapping. *Remote Sens.* **2020**, *12*, 1116. [CrossRef]
59. Donnini, M.; Marchesini, I.; Zucchini, A. Geo-LiM: A New Geo-Lithological Map for Central Europe (Germany, France, Switzerland, Austria, Slovenia, and Northern Italy) as a Tool for the Estimation of Atmospheric CO_2 Consumption. *J. Maps* **2020**, *16*, 43–55. [CrossRef]
60. Wright, W.R.; Foss, J.E. Contributions of Clay and Organic Matter to the Cation Exchange Capacity of Maryland Soils. *Soil Sci. Soc. Am. J.* **1972**, *36*, 115–118. [CrossRef]
61. Van Breemen, N.; Buurman, P. *Soil Formation*; Springer: Dordrecht, The Netherlands, 1998. [CrossRef]
62. Sikora, L.J.; Stott, D.E. Soil Organic Carbon and Nitrogen. *Methods Assess. Soil Qual.* **2015**, *49*, 157–167. [CrossRef]
63. Witzgall, K.; Vidal, A.; Schubert, D.I.; Höschen, C.; Schweizer, S.A.; Buegger, F.; Pouteau, V.; Chenu, C.; Mueller, C.W. Particulate Organic Matter as a Functional Soil Component for Persistent Soil Organic Carbon. *Nat. Commun.* **2021**, *12*, 4115. [CrossRef]
64. Gerke, J. The Central Role of Soil Organic Matter in Soil Fertility and Carbon Storage. *Soil Syst.* **2022**, *6*, 33. [CrossRef]
65. Liu, W.; Chen, S.; Qin, X.; Baumann, F.; Scholten, T.; Zhou, Z.; Sun, W.; Zhang, T.; Ren, J.; Qin, D. Storage, Patterns, and Control of Soil Organic Carbon and Nitrogen in the Northeastern Margin of the Qinghai–Tibetan Plateau. *Environ. Res. Lett.* **2012**, *7*, 035401. [CrossRef]
66. Breuer, L.; Huisman, J.A.; Keller, T.; Frede, H.G. Impact of a Conversion from Cropland to Grassland on C and N Storage and Related Soil Properties: Analysis of a 60-Year Chronosequence. *Geoderma* **2006**, *133*, 6–18. [CrossRef]
67. Enters, D.; Lücke, A.; Zolitschka, B. Effects of Land-Use Change on Deposition and Composition of Organic Matter in Frickenhauser See, Northern Bavaria, Germany. *Sci. Total Environ.* **2006**, *369*, 178–187. [CrossRef] [PubMed]
68. Mulder, C.; Hettelingh, J.P.; Montanarella, L.; Pasimeni, M.R.; Posch, M.; Voigt, W.; Zurlini, G. Chemical Footprints of Anthropogenic Nitrogen Deposition on Recent Soil C: N Ratios in Europe. *Biogeosciences* **2015**, *12*, 4113–4119. [CrossRef]
69. Matschullat, J.; Reimann, C.; Birke, M.; dos Santos Carvalho, D.; Albanese, S.; Anderson, M.; Baritz, R.; Batista, M.J.; Bel-Ian, A.; Cicchella, D.; et al. GEMAS: CNS Concentrations and C/N Ratios in European Agricultural Soil. *Sci. Total Environ.* **2018**, *627*, 975–984. [CrossRef] [PubMed]
70. Behrens, T.; Scholten, T. Digital Soil Mapping in Germany—A Review. *J. Plant Nutr. Soil Sci.* **2006**, *169*, 434–443. [CrossRef]
71. Wadoux, A.M.J.C.; Brus, D.J.; Heuvelink, G.B.M. Sampling Design Optimization for Soil Mapping with Random Forest. *Geoderma* **2019**, *355*, 113913. [CrossRef]
72. Ballabio, C.; Panagos, P.; Monatanarella, L. Mapping Topsoil Physical Properties at European Scale Using the LUCAS Database. *Geoderma* **2016**, *261*, 110–123. [CrossRef]
73. Fabian, C.; Reimann, C.; Fabian, K.; Birke, M.; Baritz, R.; Haslinger, E.; Albanese, S.; Andersson, M.; Batista, M.J.; Bel-lan, A.; et al. GEMAS: Spatial Distribution of the PH of European Agricultural and Grazing Land Soil. *Appl. Geochem.* **2014**, *48*, 207–216. [CrossRef]
74. Müller, T.S.; Dechow, R.; Flessa, H. Inventory and Assessment of PH in Cropland and Grassland Soils in Germany. *J. Plant Nutr. Soil Sci.* **2022**, *185*, 145–158. [CrossRef]
75. Potter, P.; Ramankutty, N.; Bennett, E.M.; Donner, S.D. Characterizing the Spatial Patterns of Global Fertilizer Application and Manure Production. *Earth Interact.* **2010**, *14*, 1–22. [CrossRef]
76. Tóth, G.; Guicharnaud, R.A.; Tóth, B.; Hermann, T. Phosphorus Levels in Croplands of the European Union with Implications for P Fertilizer Use. *Eur. J. Agron.* **2014**, *55*, 42–52. [CrossRef]
77. McDowell, R.W.; Noble, A.; Pletnyakov, P.; Haygarth, P.M. A Global Database of Soil Plant Available Phosphorus. *Sci. Data* **2023**, *10*, 125. [CrossRef]
78. Lilburne, L.; Helfenstein, A.; Heuvelink, G.B.M.; Eger, A. Interpreting and Evaluating Digital Soil Mapping Prediction Uncertainty: A Case Study Using Texture from SoilGrids. *Geoderma* **2024**, *450*, 117052. [CrossRef]
79. Chen, S.; Arrouays, D.; Leatitia Mulder, V.; Poggio, L.; Minasny, B.; Roudier, P.; Libohova, Z.; Lagacherie, P.; Shi, Z.; Hannam, J.; et al. Digital Mapping of GlobalSoilMap Soil Properties at a Broad Scale: A Review. *Geoderma* **2022**, *409*, 115567. [CrossRef]
80. Zanini, M.; Heiden, U.; Pace, L.; Casa, R.; Priori, S. Soil Reflectance Composite for Digital Soil Mapping in a Mediterranean Cropland District. *Remote Sens.* **2024**, *17*, 89. [CrossRef]
81. Viscarra Rossel, R.A.; Behrens, T.; Ben-Dor, E.; Chabrillat, S.; Alexandre, J.; Demattê, M.; Ge, Y.; Gomez, C.; Guerrero, C.; Peng, Y.; et al. Diffuse Reflectance Spectroscopy for Estimating Soil Properties: A Technology for the 21st Century. *Eur. J. Soil Sci.* **2022**, *73*, e13271. [CrossRef]
82. Ehlers, W.; Claupein, W. Approaches Toward Conservation Tillage in Germany. In *Conservation Tillage in Temperate Agroecosystems*; CRC Press: Boca Raton, FL, USA, 2017; pp. 141–165. [CrossRef]
83. Demattê, J.A.M.; Safanelli, J.L.; Poppiel, R.R.; Rizzo, R.; Silvero, N.E.Q.; de Mendes, W.S.; Bonfatti, B.R.; Dotto, A.C.; Salazar, D.F.U.; Mello, F.A.d.O.; et al. Bare Earth's Surface Spectra as a Proxy for Soil Resource Monitoring. *Sci. Rep.* **2020**, *10*, 4461. [CrossRef]

84. Sayão, V.M.; Demattê, J.A.M.; Bedin, L.G.; Nanni, M.R.; Rizzo, R. Satellite Land Surface Temperature and Reflectance Related with Soil Attributes. *Geoderma* **2018**, *325*, 125–140. [CrossRef]
85. de Almeida, W.S.; Panachuki, E.; de Oliveira, P.T.S.; da Silva Menezes, R.; Sobrinho, T.A.; de Carvalho, D.F. Effect of Soil Tillage and Vegetal Cover on Soil Water Infiltration. *Soil Tillage Res.* **2018**, *175*, 130–138. [CrossRef]
86. Sauer, T.J.; Horton, R. Soil Heat Flux. In *Micrometeorology in Agricultural Systems*; Wiley: Hoboken, NJ, USA, 2015; pp. 131–154. [CrossRef]
87. Amiri, R.; Weng, Q.; Alimohammadi, A.; Alavipanah, S.K. Spatial–Temporal Dynamics of Land Surface Temperature in Relation to Fractional Vegetation Cover and Land Use/Cover in the Tabriz Urban Area, Iran. *Remote Sens. Environ.* **2009**, *113*, 2606–2617. [CrossRef]
88. Song, Z.; Li, R.; Qiu, R.; Liu, S.; Tan, C.; Li, Q.; Ge, W.; Han, X.; Tang, X.; Shi, W.; et al. Global Land Surface Temperature Influenced by Vegetation Cover and PM2.5 from 2001 to 2016. *Remote Sens.* **2018**, *10*, 2034. [CrossRef]
89. Wulanningtyas, H.S.; Gong, Y.; Li, P.; Sakagami, N.; Nishiwaki, J.; Komatsuzaki, M. A Cover Crop and No-Tillage System for Enhancing Soil Health by Increasing Soil Organic Matter in Soybean Cultivation. *Soil Tillage Res.* **2021**, *205*, 104749. [CrossRef]
90. Huang, J.; Hartemink, A.E. Soil and Environmental Issues in Sandy Soils. *Earth Sci. Rev.* **2020**, *208*, 103295. [CrossRef]
91. Saffigna, P.G.; Keeney, D.R.; Tanner, C.B. Nitrogen, Chloride, and Water Balance with Irrigated Russet Burbank Potatoes in a Sandy Soil. *Agron. J.* **1977**, *69*, 251–257. [CrossRef]
92. Samuel, A.; Dines, L. *Lockhart and Wiseman's Crop Husbandry Including Grassland*; Woodhead Publishing: Sawston, UK, 2022; pp. 1–666. [CrossRef]
93. Catt, J.A. The Agricultural Importance of Loess. *Earth Sci. Rev.* **2001**, *54*, 213–229. [CrossRef]
94. Gong, J.; Chen, L.; Fu, B.; Huang, Y.; Huang, Z.; Peng, H. Effect of Land Use on Soil Nutrients in the Loess Hilly Area of the Loess Plateau, China. *Land Degrad. Dev.* **2006**, *17*, 453–465. [CrossRef]
95. Kotroczó, Z.; Fekete, I.; Juhos, K.; Prettl, N.; Nugroho, P.A.; Várbíró, G.; Biró, B.; Kocsis, T. Characterisation of Luvisols Based on Wide-Scale Biological Properties in a Long-Term Organic Matter Experiment. *Biology* **2023**, *12*, 909. [CrossRef]
96. Horn, R.; Mordhorst, A.; Fleige, H. The Impact of Arable Soil Management on Physical Functions—The Ratio of Air Capacity and Air Permeability or Hydraulic Conductivity as a Document of Harmful Soil Compaction. *Soil Tillage Res.* **2024**, *244*, 106221. [CrossRef]
97. Hartemink, A.E. Soil Fertility Decline in Some Major Soil Groupings under Permanent Cropping in Tanga Region, Tanzania. *Geoderma* **1997**, *75*, 215–229. [CrossRef]
98. Minasny, B.; McBratney, A.B.; Salvador-Blanes, S. Quantitative Models for Pedogenesis—A Review. *Geoderma* **2008**, *144*, 140–157. [CrossRef]
99. Li, J.; Du, J.; Zhong, S.; Ci, E.; Wei, C. Changes in the Profile Properties and Chemical Weathering Characteristics of Cultivated Soils Affected by Anthropic Activities. *Sci. Rep.* **2021**, *11*, 20822. [CrossRef]
100. Lal, R. Soil management in the developing countries. *Soil Sci.* **2000**, *165*, 57–72. [CrossRef]
101. Kirui, O.K. Economics of Land Degradation and Improvement in Tanzania and Malawi. In *Economics of Land Degradation and Improvement—A Global Assessment for Sustainable Development*; Springer: Cham, Switzerland, 2015; pp. 609–649. [CrossRef]
102. Nkonya, E.; Mirzabaev, A.; von Braun, J. *Economics of Land Degradation and Improvement—A Global Assessment for Sustainable Development*; Springer: Cham, Switzerland, 2015; pp. 15–32. [CrossRef]
103. Mayaki, I.; Mathai, W. We Need a Moonshot for Africa's Land Restoration Movement. 2021. Available online: https://www.wri.org/update/we-need-moonshot-africas-land-restoration-movement (accessed on 1 July 2025).
104. Hüttl, R.F.; Frielinghaus, M. Soil Fertility Problems—An Agriculture and Forestry Perspective. *Sci. Total Environ.* **1994**, *143*, 63–74. [CrossRef]
105. Seeger, M. Agricultural Soil Degradation in Germany. In *Impact of Agriculture on Soil Degradation II: A European Perspective*; Spinger: Cham, Switzerland, 2023; pp. 87–103. [CrossRef]
106. Bruckmeier, K.; Grund, H. *Agricultural Restructuring and Rural Chance in Europe*; Symes, D., Jansenm, A., Eds.; Agricultural University: Wageningen, The Netherlands, 1994.
107. Beckmann, V.; Hagedorn, K. De-Collectivisation Policies and Structural Changes of Agriculture in Eastern Germany. *MOST Econ. Policy Transitional Econ.* **1995**, *5*, 133–152. [CrossRef]
108. Panagos, P.; Jones, A.; Lugato, E.; Ballabio, C. A Soil Monitoring Law for Europe. *Glob. Chall.* **2025**, *9*, 2400336. [CrossRef] [PubMed]
109. Broothaerts, N.; Panagos, P.; Jones, A. A Proposal for Soil Health Indicators at EU-Level. 2024. Available online: https://publications.jrc.ec.europa.eu/repository/handle/JRC138417 (accessed on 1 July 2025).
110. Campbell, G.A.; Smith, P.; Broothaerts, N.; Panagos, P.; Jones, A.; Cristiano Ballabio, I.; De Rosa, D.; Lis, I.; De Jonge, W.; Arthur, E.; et al. European Journal of Soil Science Continental Scale Soil Monitoring: A Proposed Multi-Scale Framing of Soil Quality. *Eur. J. Soil Sci.* **2025**, *76*, 70174. [CrossRef]

111. Matson, A.; Fantappiè, M.; Campbell, G.A.; Miranda-Vélez, J.F.; Faber, J.H.; Carvalho Gomes, L.; Hessel, R.; Lana, M.; Mocali, S.; Smith, P.; et al. A Framework for Setting Soil Health Targets and Thresholds in Agricultural Soils. Available online: https://projects.au.dk/fileadmin/projects/ejpsoil/WP8/Policy_briefs/EJPSOIL_Policy_Brief_Targets_and_Thresholds.pdf (accessed on 1 July 2025).
112. Romero, F.; Labouyrie, M.; Orgiazzi, A.; Ballabio, C.; Panagos, P.; Jones, A.; Tedersoo, L.; Bahram, M.; Guerra, C.A.; Eisenhauer, N.; et al. Soil Health Is Linked to Primary Productivity across Europe. *bioRxiv* **2023**, bioRxiv:2023.10.29.564603.
113. Säurich, A.; Möller, M.; Gerighausen, H. A Novel Remote Sensing-Based Approach to Determine Loss of Agricultural Soils Due to Soil Sealing—A Case Study in Germany. *Environ. Monit. Assess.* **2024**, *196*, 510. [CrossRef]
114. Hannam, J.A.; Harris, M.; Deeks, L.; Hoskins, H.; Hutchison, J.; Withers, A.J.; Harris, J.A.; Way, L.; Rickson, R.J.R. Developing a Multifunctional Indicator Framework for Soil Health. *Ecol. Indic.* **2025**, *175*, 113515. [CrossRef]
115. Zeng, Y.; Verhoef, A.; Vereecken, H.; Ben-Dor, E.; Veldkamp, T.; Shaw, L.; Wang, Y.; Bob Su, Z. Tracking Soil Health: Monitoring and Modeling the Soil-Plant System. 2024. Available online: https://essopenarchive.org/doi/full/10.22541/essoar.171804479.91646868 (accessed on 1 July 2025).
116. Campbell, G.; Robinson, D.; Smith, P.; Wollesen de Jonge, L.; Nørgaard, T. Developing a Robust Soil Health Indicator Selection Framework. *Open Access Gov.* **2024**, *43*, 378–379. [CrossRef]
117. Daoud, A. Unifying Studies of Scarcity, Abundance, and Sufficiency. *Ecol. Econ.* **2018**, *147*, 208–217. [CrossRef]
118. Hartmann, T.; Wenner, F. Land Policy in Germany: Waiting for the Owner to Develop. In *Land Policies in Europe: Land-Use Planning, Property Rights, and Spatial Development*; Springer: Cham, Switzerland, 2025; pp. 121–136. [CrossRef]
119. Fischer, B.; Klauer, B.; Schiller, J. Prospects for Sustainable Land-Use Policy in Germany: Experimenting with a Sustainability Heuristic. *Ecol. Econ.* **2013**, *95*, 213–220. [CrossRef]
120. Xue, J.; Zhang, X.; Huang, Y.; Chen, S.; Dai, L.; Chen, X.; Yu, Q.; Ye, S.; Shi, Z. A Two-Dimensional Bare Soil Separation Framework Using Multi-Temporal Sentinel-2 Images across China. *Int. J. Appl. Earth Obs. Geoinf.* **2024**, *134*, 104181. [CrossRef]
121. Mayer, A.L. Strengths and Weaknesses of Common Sustainability Indices for Multidimensional Systems. *Environ. Int.* **2008**, *34*, 277–291. [CrossRef] [PubMed]
122. Ballabio, C.; Lugato, E.; Fernández-Ugalde, O.; Orgiazzi, A.; Jones, A.; Borrelli, P.; Montanarella, L.; Panagos, P. Mapping LUCAS Topsoil Chemical Properties at European Scale Using Gaussian Process Regression. *Geoderma* **2019**, *355*, 113912. [CrossRef] [PubMed]
123. Reidsma, P.; Janssen, S.; Jansen, J.; van Ittersum, M.K. On the Development and Use of Farm Models for Policy Impact Assessment in the European Union—A Review. *Agric. Syst.* **2018**, *159*, 111–125. [CrossRef]
124. Orgiazzi, A.; Ballabio, C.; Panagos, P.; Jones, A.; Fernández-Ugalde, O. LUCAS Soil, the Largest Expandable Soil Dataset for Europe: A Review. *Eur. J. Soil Sci.* **2018**, *69*, 140–153. [CrossRef]
125. Panagos, P.; Van Liedekerke, M.; Borrelli, P.; Köninger, J.; Ballabio, C.; Orgiazzi, A.; Lugato, E.; Liakos, L.; Hervas, J.; Jones, A.; et al. European Soil Data Centre 2.0: Soil Data and Knowledge in Support of the EU Policies. *Eur. J. Soil Sci.* **2022**, *73*, e13315. [CrossRef]
126. Viscarra Rossel, R.A.; Adamchuk, V.I.; Sudduth, K.A.; McKenzie, N.J.; Lobsey, C. Proximal Soil Sensing. An Effective Approach for Soil Measurements in Space and Time. *Adv. Agron.* **2011**, *113*, 237–282. [CrossRef]
127. Ahrends, H.E.; Simojoki, A.; Lajunen, A. Spatial Pattern Consistency and Repeatability of Proximal Soil Sensor Data for Digital Soil Mapping. *Eur. J. Soil Sci.* **2023**, *74*, e13409. [CrossRef]

Disclaimer/Publisher's Note: The statements, opinions and data contained in all publications are solely those of the individual author(s) and contributor(s) and not of MDPI and/or the editor(s). MDPI and/or the editor(s) disclaim responsibility for any injury to people or property resulting from any ideas, methods, instructions or products referred to in the content.